40 Shaw T, Bartholomeusz A, Locarnini S. HBV drug resistance: mechanisms, detection and interpretation. *J Hepatol* 2006; 44: 593–606.
41 Marcellin P, Chang TT, Lim SG *et al.* Adefovir dipivoxil for the treatment of hepatitis B e antigen-positive chronic hepatitis B. *N Engl J Med* 2003; 348: 808–816.
42 Santantonio T, Fasano M, Durantel S *et al.* Adefovir dipivoxil resistance patterns in patients with lamivudine-resistant chronic hepatitis B. *Antivir Ther* 2009; 14: 557–565.
43 Qi X, Xiong S, Yang H, Miller M, Delaney WE. In vitro susceptibility of adefovir-associated hepatitis B virus polymerase mutations to other antiviral agents. *Antivir Ther* 2007; 12: 355–362.
44 Tan J, Degertekin B, Wong SN, Husain M, Oberhelman K, Lok AS. Tenofovir monotherapy is effective in hepatitis B patients with antiviral treatment failure to adefovir in the absence of adefovir-resistant mutations. *J Hepatol* 2008; 48: 391–398.
45 van Bommel F, Zollner B, Sarrazin C *et al.* Tenofovir for patients with lamivudine-resistant hepatitis B virus (HBV) infection and high HBV DNA level during adefovir therapy. *Hepatology* 2006; 44: 318–325.
46 Choe WH, Kwon SY, Kim BK *et al.* Tenofovir plus lamivudine as rescue therapy for adefovir-resistant chronic hepatitis B in hepatitis B e antigen-positive patients with liver cirrhosis. *Liver Int* 2008; 28: 814–820.
47 Lok AS, McMahon BJ. Chronic hepatitis B. *Hepatology* 2007; 45: 507–539.

SUPPORTING INFORMATION

Additional Supporting Information may be found in the online version of this article:

Table S1 Clonal analysis of HBV RT region of samples from the patient with lamivudine and adefovir resistance.

Please note: Wiley-Blackwell are not responsible for the content or functionality of any supporting materials supplied by the authors. Any queries (other than missing material) should be directed to the corresponding author for the article.

Activation of Alpha$_1$-Adrenergic Receptors Stimulate the Growth of Small Mouse Cholangiocytes Via Calcium-Dependent Activation of Nuclear Factor of Activated T Cells 2 and Specificity Protein 1

Gianfranco Alpini,[1,2,3]* Antonio Franchitto,[5]* Sharon DeMorrow,[2,3] Paolo Onori,[6] Eugenio Gaudio,[5] Candace Wise,[2,3] Heather Francis,[2,3,4] Julie Venter,[2,3] Shelley Kopriva,[2,3] Romina Mancinelli,[3,5] Guido Carpino,[7] Franco Stagnitti,[9] Yoshiyuki Ueno,[8] Yuyan Han,[2,3] Fanyin Meng,[2,3,4] and Shannon Glaser[2,3]

Small cholangiocytes proliferate via activation of calcium (Ca^{2+})-dependent signaling in response to pathological conditions that trigger the damage of large cyclic adenosine monophosphate–dependent cholangiocytes. Although our previous studies suggest that small cholangiocyte proliferation is regulated by the activation of Ca^{2+}-dependent signaling, the intracellular mechanisms regulating small cholangiocyte proliferation are undefined. Therefore, we sought to address the role and mechanisms of action by which phenylephrine, an α_1-adrenergic agonist stimulating intracellular D-*myo*-inositol-1,4,5-triphosphate (IP_3)/Ca^{2+} levels, regulates small cholangiocyte proliferation. Small and large bile ducts and cholangiocytes expressed all AR receptor subtypes. Small (but not large) cholangiocytes respond to phenylephrine with increased proliferation via the activation of IP_3/Ca^{2+}-dependent signaling. Phenylephrine stimulated the production of intracellular IP_3. The Ca^{2+}-dependent transcription factors, nuclear factor of activated T cells 2 (NFAT2) and NFAT4, were predominantly expressed by small bile ducts and small cholangiocytes. Phenylephrine stimulated the Ca^{2+}-dependent DNA-binding activities of NFAT2, NFAT4, and Sp1 (but not Sp3) and the nuclear translocation of NFAT2 and NFAT4 in small cholangiocytes. To determine the relative roles of NFAT2, NFAT4, or Sp1, we knocked down the expression of these transcription factors with small hairpin RNA. We observed an inhibition of phenylephrine-induced proliferation in small cholangiocytes lacking the expression of NFAT2 or Sp1. Phenylephrine stimulated small cholangiocyte proliferation is regulated by Ca^{2+}-dependent activation of NFAT2 and Sp1. *Conclusion:* Selective stimulation of Ca^{2+}-dependent small cholangiocyte proliferation may be key to promote the repopulation of the biliary epithelium when large bile ducts are damaged during cholestasis or by toxins. (HEPATOLOGY 2011;53:628-639)

In human and experimental cholangiopathies, the proliferation/loss of bile ducts is restricted to specific-sized bile ducts.[1-3] The secretory and proliferative capacity of large cholangiocytes depends on the activation of adenosine 3′,5′-monophosphate (cAMP)-dependent mechanisms.[2-4] Large (but not small)

Abbreviations: AR, adrenergic receptor; $[Ca^{2+}]_i$, intracellular calcium; BAPTA/AM, 1,2-bis-(o-aminophenoxy)-ethane-N,N,N′,N′-tetraacetic acid, tetraacetoxymethyl ester; BMY 7378 dihydrochloride, 8-[2-[4-(2-methoxyphenyl)-1-piperazinyl]ethyl]-8-azaspiro[4.5]decane-7,9-dione dihydrochloride; BRL 37344, (±)-(R,R*)-[4-[2-[[2-(3-chlorophenyl)-2-hydroxyethyl]amino]propyl]phenoxy]acetic acid; BSA, bovine serum albumin; CAI, calcineurin autoinhibitory peptide; cAMP, 3′-5′-cyclic adenosine monophosphate; CaMK, calmodulin-dependent protein kinase; CK-19, cytokeratin-19; clen, clenbuterol; $\Delta\Delta C_T$, delta delta of the threshold cycle; dobut, dobutamine; EMSA, electrophoretic mobility shift assay; IBDM, intrahepatic bile duct mass; IP_3, D-myo-inositol-1,4,5-triphosphate; MiA, mithramycin A; MTS, 3-(4,5-dimethylthiazol-2-yl)-5-(3-carboxymethoxyphenyl)-2-(4-sulfophenyl)-2H-tetrazolium, inner salt; NFAT, nuclear factor of activated T cells; PCR, polymerase chain reaction; phenyl, phenylephrine; Rec 15/2615 dihydrochloride, 1-(4-amino-6,7-dimethoxy-2-quinazolinyl)-4-[[2-methoxy-6-(1-methylethyl)phenoxy]acetyl]piperazine dihydrochloride; RS-17053, N-[2-(2-cyclopropylmethoxyphenoxy)ethyl]-5-chloro-alpha, alpha-dimethyl-1H-indole-3-ethanamine hydrochloride; Sp1/3, specificity protein 1/3.*

From the [1]Central Texas Veterans Health Care System, [2]Scott & White Digestive Disease Research Center, [3]Department of Medicine, Division Gastroenterology, Texas A&M Health Science Center, College of Medicine, [4]Division of Research and Education at Scott & White, Temple, TX, [5]Department of Human Anatomy and [9]Department of Surgery, University of Rome "La Sapienza", Rome, Italy; [6]Department of Experimental Medicine, University of L'Aquila, L'Aquila, Italy, [7]Department of Health Science, "Foro Italico" University of Rome, Italy; and [8]Division of Gastroenterology, Tohoku University School of Medicine, Sendai, Japan.

Received June 5, 2010; accepted October 1, 2010.

cholangiocytes are more susceptible to toxins (e.g., carbon tetrachloride [CCl_4]) that induce the loss of proliferative and secretory activity.[3] Immortalized small cholangiocyte lines[5] proliferate via D-myo-inositol 1,4,5-triphosphate (IP_3)/Ca^{2+}/calmodulin-dependent protein kinase (CaMK) I–dependent mechanisms regulated via activation of H1 histamine receptor subtypes.[6] Ca^{2+}-dependent small cholangiocyte proliferation may be a key compensatory mechanism for maintaining homeostasis and overall bile duct function in pathological ductopenic conditions associated with damage of large ducts.[3,7]

We have demonstrated that: (1) cholangiocytes express adrenergic receptors (ARs) including $\alpha_{1A/1C}$, α_{1B}, α_{2A}, α_{2B}, α_{2C}, β_1, and β_2 subtypes; and (2) administration of agonists for these receptors regulate large cholangiocyte function by modulation of cAMP-dependent signaling.[8-10] For example, activation of $\alpha_{1A/1C}$, α_{1B} AR (by phenylephrine) stimulates secretin-stimulated cholangiocyte choleresis of bile duct–ligated rats via Ca^{2+}-dependent stimulation of cAMP signaling.[10] The expression of α_1-AR receptors, which are G-protein–coupled receptors signaling via Ca^{2+},[11] in small and large cholangiocytes and the possible effects of their stimulation on proliferation has not been explored. In particular, activation of Ca^{2+}-dependent signaling in small cholangiocytes by AR agonists, such as phenylephrine, that are known to trigger intracellular Ca^{2+} signaling,[10] has not been studied.

Nuclear factor of activated T cells (NFAT) is a ubiquitous transcription factor initially described in T-lymphocytes. Five NFAT family members have been described: NFAT1 (also known as NFATp or NFATc2), NFAT2 (NFATc or NFATc1), NFAT3, NFAT4 (NFATx or NFATc3), and NFAT5.[12] NFAT1, NFAT2, NFAT3, and NFAT4 are regulated by calcium/calcineurin signaling,[13] whereas activation of NFAT5 is calcineurin independent.[14] In nonstimulated cells, NFAT proteins are located in the cytoplasm in a hyper-phosphorylated state. Following increases in $[Ca^{2+}]_i$, the Ca^{2+}/calmodulin-dependent serine/threonine phosphatase, calcineurin, directly dephosphorylates NFAT, which induces rapid nuclear import providing a direct link between $[Ca^{2+}]_i$ signaling and gene expression.[13] In the nucleus, NFAT proteins bind to target promoter elements alone or in combination with other nuclear elements such as Sp1/Sp3 to regulate gene transcription. Nevertheless, the potential role of Ca^{2+}/calcineurin dependent activation of NFAT in the regulation of small cholangiocyte proliferation has not been addressed.

Materials and Methods

Materials. Reagents were obtained from Sigma Chemical Co. (St. Louis, MO) unless otherwise indicated. The mouse monoclonal antibodies for NFAT1 and NFAT2 were purchased from Novus Biologicals, Inc. (Littleton, CO). The rabbit polyclonal antibody for NFAT3 and the mouse monoclonal antibody for NFAT4 were purchased from Santa Cruz Biotechnology (Santa Cruz, CA). The radioimmunoassay kits for the determination of intracellular cAMP (cAMP [^{125}I] Biotrak Assay System) and IP_3 (IP_3 [^{3}H] Biotrak Assay System) levels were purchased from GE Healthcare (Piscataway, NJ).

Immortalized and Freshly Isolated Small and Large Cholangiocytes. Small and large cholangiocytes from normal mice (BALB/c) were immortalized by the introduction of the simian virus-40 large T antigen gene[5] and cultured as described.[6] These cell lines display morphological, phenotypic and functional features similar to freshly isolated small and large mouse cholangiocytes.[5,6,15] Freshly isolated small and large mouse cholangiocytes were purified as described.[2,6,15-17]

Animal Models. Male C57/Bl6N mice (20-25 g) were purchased from Charles River (Wilmington, MA). Animals received humane care according to the "Guide for the Care and Use of Laboratory Animals" prepared by the National Academy of Sciences and published by

*These authors contributed equally to this article.

Supported by This work was supported partly by the Dr. Nicholas C. Hightower Centennial Chair of Gastroenterology from Scott & White, the VA Research Scholar Award, a VA Merit Award and National Institutes of Health (NIH) grants DK58411, and DK76898 to Dr. Alpini, an NIH RO1 grant award to Dr. Glaser (DK081442) an NIH K01 grant award (DK078532) to Dr. DeMorrow, and by University funds to Dr. Onori and PRIN 2007 (# 2007HPT7BA_001) and Federate Athenaeum funds from University of Rome "La Sapienza" to Prof. Gaudio and by a grant-in-aid for Scientific Research (C) from Japan Promotion of Science (21590822), and by Health and Labour Sciences Research Grants for the Research on Measures for Intractable Diseases (from the Ministry of Health, Labour and Welfare of Japan) to Dr. Ueno.

Address reprint requests to: Shannon Glaser, Ph.D., or Gianfranco Alpini, Ph.D., 702 SW H.K. Dodgen Loop, Temple, TX, 76504. E-mail: galpini@tamu.edu (G.A.) or sglaser@medicine.tamhsc.edu (S.G.); fax: 254-724-9278.

View this article online at wileyonlinelibrary.com.

DOI 10.1002/hep.24041

Potential conflict of interest: Nothing to report.

Additional Supporting Information may be found in the online version of this article.

the National Institutes of Health. Normal mice were treated with saline or phenylephrine (10 mg/kg body weight, daily intraperitoneal injections)[18] for 1 week in the absence/presence of: (1) 11R-VIVIT, a cell-permeable NFAT inhibitor peptide, 10 mg/kg, daily intraperitoneal injections; or (2) mithramycin A (MiA), an Sp1 inhibitor, 0.5 mg/kg, intraperitoneal injections twice weekly)[19,20] before evaluating intrahepatic bile duct mass (IBDM, by immunohistochemistry for cytokeratin-19 [CK-19])[21] of small and large bile ducts. Stained sections were analyzed for each group using a BX-51 light microscopy (Olympus, Tokyo, Japan).

Expression of Adrenergic Receptors. The expression of α_{1A}, α_{1B}, α_{1D}-AR was evaluated by: (1) immunohistochemistry in liver sections and (2) immunofluorescence and fluorescence-activated cell sorting (FACS) analysis in immortalized small and large cholangiocytes. We evaluated the presence of the message for α_{1A}, α_{1B}, α_{1D}, α_{2A}, α_{2B}, α_{2C}, β_1, β_2, and β_3, AR by real-time polymerase chain reaction (PCR) in freshly isolated and immortalized small and large cholangiocytes. Immunohistochemistry was performed in paraffin-embedded liver sections (4-5 μm thickness).[6] Light microscopy photographs of 10 non-overlapping fields liver sections were evaluated for receptor expression. Immunofluorescence in cell smears was performed as described.[6] Negative controls were performed by usage of a pre-immune serum instead of the primary antibody. FACS analysis was performed as described[22] using a C6 flow cytometer (Accuri, Inc., Ann Arbor, MI) and analyzed by CFlow Software. At least 20,000 events in the light-scatter (side scatter/forward scatter) were acquired. AR receptors were identified and gated on FL1-A/Count plots. The relative quantity of AR (mean AR fluorescence) was expressed as mean FL1-A (samples)/mean FL-1A (secondary antibodies only). For real-time PCR, a $\Delta\Delta C_T$ (delta delta of the threshold cycle) analysis was performed.[23] The primers for α_{1A}, α_{1B}, α_{1D}, α_{2A}, α_{2B}, α_{2C}, β_1, β_2 and β_3 AR subtypes were designed by SABiosciences (Frederick, MD) according to the sequences listed in the National Center for Biotechnology Information. Data were expressed as fold-change of the ratio of relative messenger RNA levels ± standard error of the mean of AR to glyceraldehyde-3-phosphate dehydrogenase (GAPDH).

Expression of NFAT Isoforms. The expression of the different NFAT isoforms (NFAT1, NFAT2, NFAT3, and NFAT4) was evaluated by: (1) immunohistochemistry in normal liver sections[6]; and (2) immunofluorescence in immortalized small and large cholangiocytes.[6] In liver sections, when 0%-5% of bile ducts were positive for NFAT isoforms, we assigned a negative score; a +/− score was assigned when 6%-10% of bile ducts were positive; a + score was assigned when 11%-30% of bile ducts were positive; and a ++ score was assigned with 31%-60% of bile ducts positive.[15]

Effect of Adrenergic Receptor Agonists on the Proliferation of Immortalized Small and Large Cholangiocytes. The effect of phenylephrine on small cholangiocyte proliferation was evaluated at varying dosages (10^{-11} to 10^{-3} M) and times (24-72 hours) by MTS [3-(4,5-dimethylthiazol-2-yl)-5-(3-carboxymethoxyphenyl)-2-(4-sulfophenyl)-2H-tetrazolium, inner salt] proliferation assay.[6] The effects (24 hours at 37°C) of α_1 (phenylephrine, 10 μM),[10] α_2 (UK14,304, 50 μM),[8] β_1 (dobutamine, 10 μM),[9,10] β_2 (clenbuterol, 10 μM)[9] or β_3 (BRL 37344, 10 μM)[24] AR agonists on the proliferation of small and large cholangiocytes were evaluated by MTS proliferation assays.[6] The concentration of 10 μM for phenylephrine was chosen based on the fact that: (1) at this concentration (10 μM) phenylephrine stimulates cholangiocyte secretory activity[10]; and (2) the doses (10^{-11} to 10^{-5} M) used for phenylephrine induced a similar increase in small cholangiocyte proliferation (Fig. 3A). Because phenylephrine was the only α_1-AR agonist to increase small cholangiocyte proliferation (see results section), in separate sets of experiments we evaluated by MTS assay[6] the effect of phenylephrine on small cholangiocyte proliferation in the absence or presence of: (1) BAPTA/AM (intracellular Ca^{2+} chelator, 5 μM)[6]; (2) CAI (calcineurin autoinhibitory peptide, 50 μM)[4]; (3) 11R-VIVIT (1 nM)[19]; or (4) MiA (50 nM).[25] To demonstrate that the effects of phenylephrine on cholangiocyte proliferation are due to selective interaction with α-1 AR, we evaluated the effect of phenylephrine (10 μM for 24 hours) on the proliferation of small cholangiocytes in the absence or presence of: (1) RS-17053 (selective α_{1A}-AR antagonist, 1 nM)[26]; (2) Rec 15/2615 dihydrochloride (selective α_{1B}-AR antagonist, 10 nM)[27]; or (3) BMY 7378 dihydrochloride (selective α_{1D}-AR antagonist, 1 nM).[28]

Effect of Phenylephrine on Intracellular cAMP and IP3 Levels. Immortalized small and large cholangiocytes were stimulated at room temperature for 5 minutes with 0.2% bovine serum albumin (BSA; basal) or phenylephrine (10 μM in 0.2% BSA).[10] Intracellular cAMP and IP_3 levels were measured by commercially available kits according to the instructions provided by the vendor.

Effect of Phenylephrine on the Nuclear Translocation and DNA-Binding Activity of NFAT2, NFAT4, Sp1, and Sp3 of Immortalized Small Cholangiocytes. Experiments were performed to evaluate the effect of phenylephrine on: (1) the nuclear

translocation of NFAT2 and NFAT4, the isoforms expressed by immortalized small cholangiocytes by immunofluorescence; and (2) NFAT2, Sp1, and Sp3 DNA-binding activity by enzyme-linked immunosorbent assay (ELISA)[29] and electrophoretic mobility shift assay (EMSA)[30] in immortalized small cholangiocytes. Nuclear translocation of NFAT2 and NFAT4 was evaluated by immunofluorescence[6] in small cholangiocytes treated with 0.2% BSA or phenylephrine (10 μM in 0.2% BSA) for 1 hour at 37°C in the presence/absence of pretreatment for 30 minutes with benoxathian (nonsubtype selective α_1-AR antagonist, 50 μM),[31] BAPTA/AM or CAI. NFAT2 (a kit is not available for NFAT4), Sp1, and Sp3 DNA-binding activity was measured by a commercially available ELISA-based kit that detects transcription factor activation (TransAM transcription factor assay kit; Active Motif, Carlsbad, CA). Immortalized small cholangiocytes were stimulated with 0.2% BSA (basal) or phenylephrine (10 μM in 0.2% BSA) for 1 hour at 37°C in the presence/absence of BAPTA/AM, or CAI or MiA. Nuclear extracts were analyzed transcription for factor activation according to the manufacturer's protocol (Active Motif, Carlsbad, CA). The relative DNA-binding of NFAT2/4 and Sp1was assessed by EMSA in immortalized small cholangiocytes treated with phenylephrine (10 μM) for 0-minute, 30-minute, and 60-minute timepoints at 37°C as described.[30] Double-stranded oligonucleotides containing either the consensus binding motif for NFAT (Santa Cruz Biotechnology), Sp1 (Promega, Madison, WI) or Oct (Promega) were end-labeled with [^{32}P]deoxyadenosine triphosphate using T4 polynucleotide kinase for 10 minutes at room temperature. The NFAT consensus sequence binds both NFAT2 and NFAT4 isoforms.[32] In parallel, to prove specificity of the relevant DNA-binding activities, cold competition assays were performed by adding 50-fold excess of unlabeled consensus sequences for NFAT, a mutant NFAT sequence that differs from the native sequence by three base pairs (Santa Cruz Biotechnology), Oct or Sp1 prior to the addition of the labeled sequence.

Knockdown of NFAT2, NFAT4, and Sp1 Expression in Immortalized Small Cholangiocytes. Immortalized small cholangiocyte cell lines lacking NFAT2, NFAT4 and Sp1 expression were established using SureSilencing short hairpin RNA (shRNA; SuperArray, Frederick, MD) plasmids for mouse NFAT2, NFAT4 and Sp1, containing neomycin (for NFAT2) and puromycin (for NFAT4 and Sp1) resistance for the selection of stably transfected cells, according to the instructions provided by the vendor.[33] Approximately 70% knockdown of NFAT2, NFAT4, and Sp1 messenger RNA expression was achieved in immortalized small cholangiocytes (Supporting Information Fig. 1A). Immunofluorescence and DNA-binding activity for NFAT2, NFAT4, and Sp1 by EMSA were used to validate the knockdown of protein expression in small cholangiocytes (Supporting Information Fig. 1B). There was no inadvertent knockdown of NFAT2, NFAT4, and Sp1 in each case. The small cholangiocyte cell line, mock-transfected clone (Neo-Control shRNA or Puro-Control shRNA), the NFAT2 knockdown clone, NFAT4 knockdown clone, and the Sp1 knockdown clone were stimulated with 0.2% BSA (basal) or phenylephrine (10 mM in 0.2% BSA) for 24 hours before evaluation of proliferation by MTS assays.[6]

Results

Cholangiocytes Express α1-AR Subtypes. In normal liver sections, we demonstrated that α_{1A}, α_{1B}, α_{1D}-AR are expressed by small (yellow arrow) and large (red arrow) bile ducts (Fig. 1A). Immortalized small and large cholangiocytes were positive for α_{1A}, α_{1B}, α_{1D}-AR expression (Fig. 1B). By real-time PCR, freshly isolated and immortalized small and large cholangiocytes express the messages for α_{1A}, α_{1B}, α_{1D}, α_{2A}, α_{2B}, α_{2C}, β_1, β_2, and β_3 AR (Supporting Information Fig. 2A). By FACS, we demonstrated that immortalized small and large cholangiocytes express the protein for α_{1A}, α_{1B}, α_{1D}-AR (Supporting Information Fig. 2B).

Small Bile Ducts and Cholangiocytes Express NFAT2 and NFAT4. By immunohistochemistry, small bile ducts in liver sections express the NFAT2 and NFAT4 isoforms (Fig. 2A). Large bile ducts in liver sections expressed lower levels of NFAT2 and NFAT4 (Fig. 2A) as determined by semiquantitative immunohistochemical analysis (Supporting Information Table 1). By immunofluorescence, we demonstrated that NFAT2 and NFAT4 were predominantly expressed by immortalized small cholangiocytes and that NFAT3 was expressed by large cholangiocytes (Fig. 2B). NFAT1 was not expressed by small or large bile ducts or immortalized small and large cholangiocytes (Fig. 2A,B).

Phenylephrine Stimulates In Vivo and In Vitro the Proliferation of Small but not Large Cholangiocytes. Chronic *in vivo* administration of phenylephrine to normal mice induces a significant increase in IBDM of small cholangiocytes, increase that was blocked by 11R-VIVIT and mithramycin A (Fig. 3). The *in vitro* doses (10^{-11} to 10^{-5} M) used for phenylephrine induced a similar increase in the proliferation of immortalized small

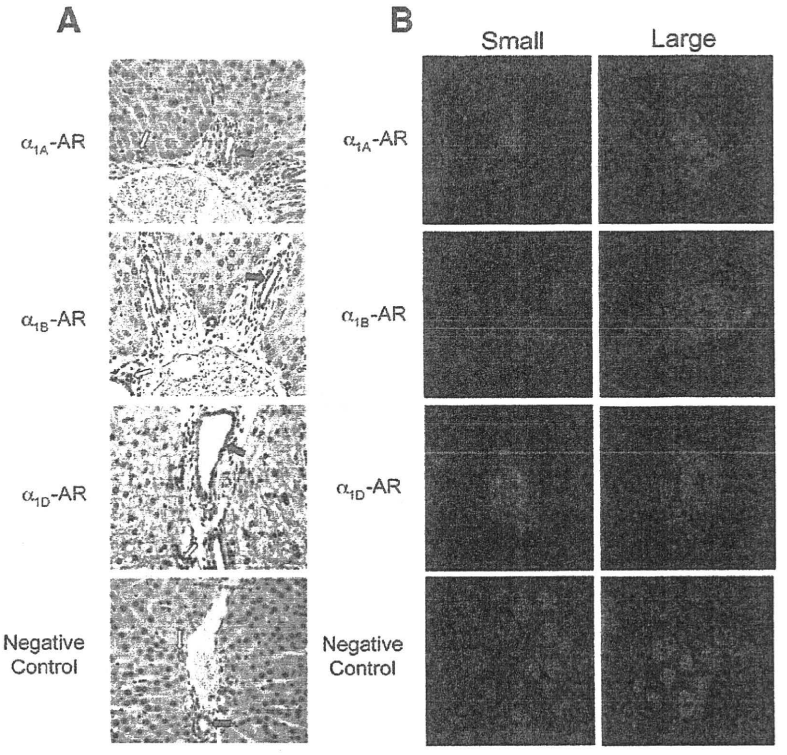

Fig. 1. Expression of α_{1A}, α_{1B}, α_{1D} AR by immunohistochemistry (A) in liver sections, and immunofluorescence (B) in immortalized small and large cholangiocytes. (A) Small (yellow arrows) and large (red arrows) bile ducts were positive for α_{1A}-, α_{1B}-, and α_{1D}-AR expression. Original magnification, ×20. (B) Immortalized small and large cholangiocytes were positive for α_{1A}-, α_{1B}-, and α_{1D}-AR. AR expression is shown in red with nuclei counterstained with DAPI (4′,6-diamidino-2-phenylindole; blue). Original magnification, ×60. The negative control performed without the primary antibody is presented at the bottom of the figure. Bile ducts (A) and immortalized small and large cholangiocytes (B) express α_{1A}, α_{1B}, and α_{1D}-AR.

cholangiocytes (Fig. 4A). To determine the potential role of each of the AR subtypes on the proliferation of immortalized small and large cholangiocytes, we performed MTS proliferation assays in the presence/absence of α_1 (phenylephrine), α_2 (UK14,304), β_1 (dobutamine), β_2 (clenbuterol) or β_3 (BRL 37344) AR agonists. In large cholangiocytes, we observed that dobutamine, clenbuterol, and BRL 37344 stimulated proliferation, whereas phenylephrine and UK14,304 had no effect on the growth of large cholangiocytes (Fig. 4B). In addition to phenylephrine, dobutamine (but not clenbuterol, and BRL 37344) increased small cholangiocyte proliferation (Fig. 4B). Because activation of β-adrenergic receptors regulates biliary functions by increased intracellular cAMP levels in cholangiocytes,[9] we focused our studies on the role of phenylephrine (an α_1-AR agonist stimulating IP_3/Ca^{2+} levels)[10,34] on Ca^{2+}-dependent signaling in small cholangiocytes. We demonstrated that α_{1A} (RS17053), α_{1B} (Rec15/2615) and α_{1D} (BMY7378) AR antagonists induced a partial yet significant reduction in phenylephrine-induced proliferation of immortalized small cholangiocytes (Fig. 4C). However, levels of proliferation stimulated by phenylephrine in the presence of the antagonists remain significant in comparison to basal control proliferation, which demonstrates that all three receptor subtypes are involved in phenylephrine-induced proliferation (Fig. 4C).

Phenylephrine Stimulates the Proliferation of Immortalized Small Cholangiocytes Via Ca2+-Dependent Signaling Mechanism. Phenylephrine increased intracellular IP_3 (but not cAMP, not shown) levels (basal: 0.39 ± 0.03 versus phenylephrine: 0.62 ± 0.07 pmol/1 × 10^7 cells; $P < 0.01$) in immortalized small cholangiocytes. Phenylephrine-stimulated proliferation of immortalized small cholangiocytes was blocked by BAPTA/AM, CAI,[4] 11R-VIVIT, and MiA (Fig. 4D).

Phenylephrine Stimulates the Nuclear Translocation of NFAT and DNA-Binding Activity of NFAT2/4 and Sp1 in Immortalized Small Cholangiocytes. To further define the role of NFAT in phenylephrine-stimulated proliferation, we performed experiments to evaluate nuclear translocation and DNA-binding activity of NFAT2 and NFAT4 in immortalized small cholangiocytes. By immunofluorescence, phenylephrine stimulates nuclear translocation of both NFAT2 and NFAT4 in small cholangiocytes (Fig. 5). This translocation that was blocked by inhibitors of upstream Ca^{2+}-dependent signaling (i.e., benoxathian [nonsubtype selective α_1-AR antagonist],[31] BAPTA/AM, and CAI) (Fig. 5), which confirms the results of the proliferation studies (Fig. 4D). The activation of NFAT and Sp1/3 DNA-binding activity was determined by EMSA and DNA-binding activity ELISA. We found by EMSA that phenylephrine stimulates time-dependent activation of NFAT

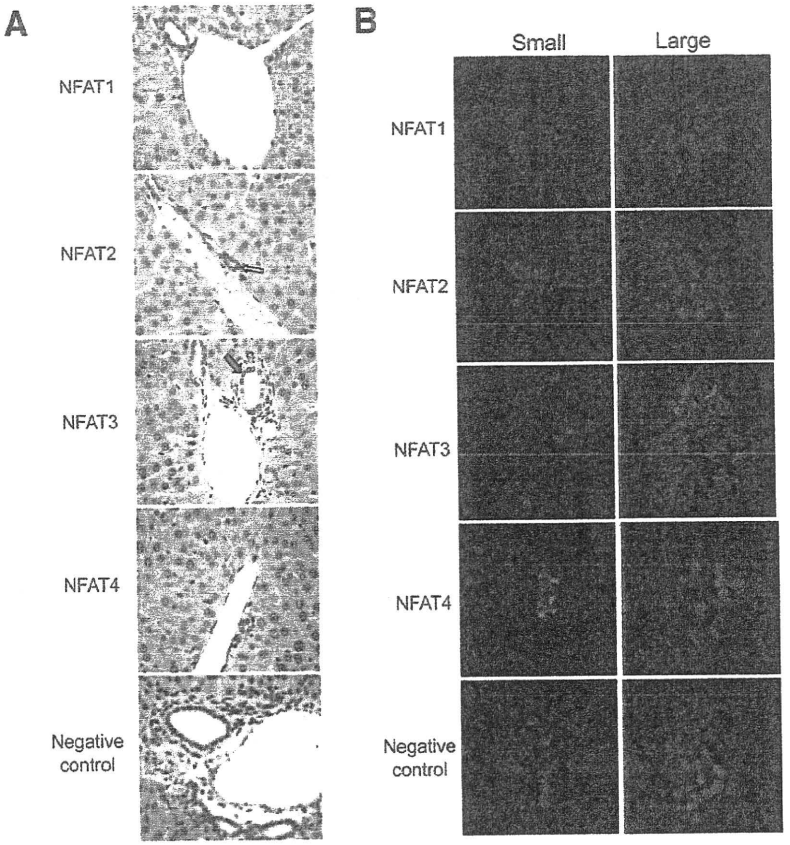

Fig. 2. Expression of NFAT isoforms by immunohistochemistry (A) in liver sections, and immunofluorescence (B) in immortalized small and large cholangiocytes. (A) NFAT2 and 4 were expressed predominantly by small bile ducts (yellow arrows; for semiquantitative data see Supporting Information Table 1). A small percent of cholangiocytes in large bile ducts (red arrows) stained positively for NFAT2 and 4. NFAT3 was expressed only in large bile ducts, whereas NFAT1 was not expressed in either sized bile ducts. Original magnification, ×20. (B) A similar expression profile was observed in immortalized small and large cholangiocytes. Small cholangiocytes were positive for NFAT2 and 4. Large cholangiocytes were positive for NFAT3, whereas neither cell type expressed NFAT1. Original magnification, ×60. A representative negative control performed without the primary antibody is presented at the bottom of the figure.

DNA-binding in small cholangiocytes (Fig. 6). The consensus sequence used in the EMSA will bind both NFAT2 and NFAT4 (elucidation of the involvement of isoforms was determined by knockdown experiments discussed later). NFAT2 DNA-binding activity was confirmed by DNA-binding activity ELISA. The ELISA kit used recognizes the specific DNA-binding activity of NFAT2 (and not other NFAT isoforms as

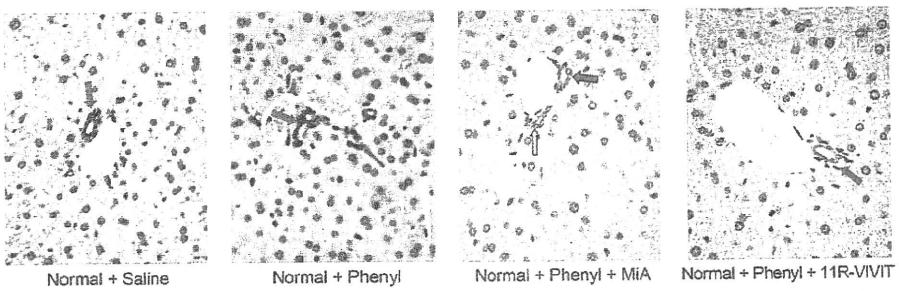

	Intrahepatic Bile Duct Mass (% surface)			
	Normal + Saline	Normal + Phenyl	Normal + Phenyl + MiA	Normal + Phenyl + 11R-VIVIT
Small Ducts	0.042 ± 0.007	0.092 ± 0.012*	0.052 ± 0.005	0.053 ± 0.004
Large Ducts	0.163 ± 0.005	0.163 ± 0.007	0.168 ± 0.009	0.167 ± 0.008

Fig. 3. Expression of CK-19 by immunohistochemistry in liver sections of normal mouse treated with vehicle or phenylephrine for 1 week in the absence or presence of 11R-VIVIT or MiA. Large (red arrow) and small (yellow arrows) ducts are indicated. Original magnification, ×40. Measurement of IBDM of small and large cholangiocytes in liver sections from the selected groups of mice. Chronic administration of phenylephrine to normal mice induces a significant increase in IBDM of small but not large cholangiocytes, increase that was blocked by 11R-VIVIT and MiA. *$P = 0.0022$ (by Mann-Whitney test) versus IBDM of small cholangiocytes from normal mice treated with phenylephrine versus normal mice treated with vehicle.

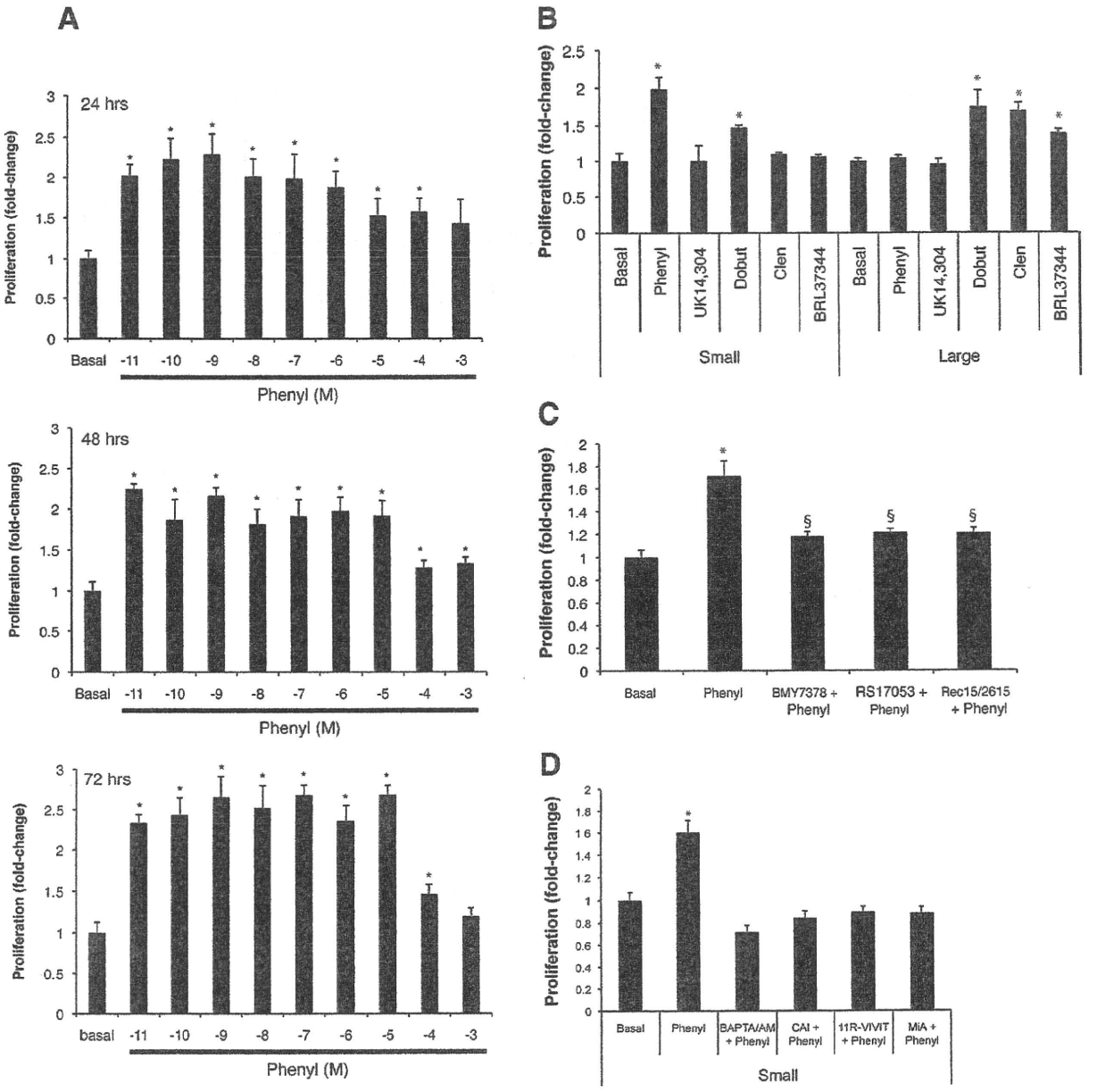

Fig. 4. (A) Effect of different doses (10^{-11} to 10^{-3} M) of phenylephrine on the proliferation of immortalized small cholangiocytes. The doses (10^{-11} to 10^{-5} M) used for phenylephrine induced a similar increase in small cholangiocyte proliferation. Asterisk (*) denotes significance ($P < 0.05$) when compared with the respective basal treatment using a Kruskal-Wallis test (n = 6-14). (B) In addition to phenylephrine, dobutamine increased small cholangiocyte proliferation. In immortalized large cholangiocytes, dobutamine, clenbuterol and BRL 37344 induced a significant increase in proliferation, whereas phenylephrine and UK14,304 had no effect. Asterisk (*) denotes significance ($P < 0.05$) when compared with the respective basal treatment using a Kruskal-Wallis test (n = 14). (C) Effect of phenylephrine (10 μM for 24 hours) on the proliferation of immortalized small cholangiocytes in the absence or presence of selective AR antagonists. α_{1A}-, α_{1B}-, and α_{1D}-AR antagonists induced a partial yet significant reduction in phenylephrine-induced small cholangiocyte proliferation. Asterisk (*) denotes significance ($P < 0.05$) when compared with the respective basal treatment using a *t* test (n = 14). Section symbol (§) denotes significance ($P < 0.05$) when compared with phenylephrine-induced proliferation. (D) Phenylephrine stimulates small cholangiocytes proliferation in a Ca^{2+}-dependent mechanism. Small mouse cholangiocytes were stimulated with phenylephrine in the presence/absence of BAPTA/AM, CAI, 11R-VIVIT, or MiA. Phenylephrine-stimulated small cholangiocyte proliferation was prevented by BAPTA/AM, CAI, 11R-VIVIT, or MiA. Asterisk (*) denotes significance ($P < 0.05$) when compared with the respective basal treatment using a Kruskal-Wallis test (n = 14).

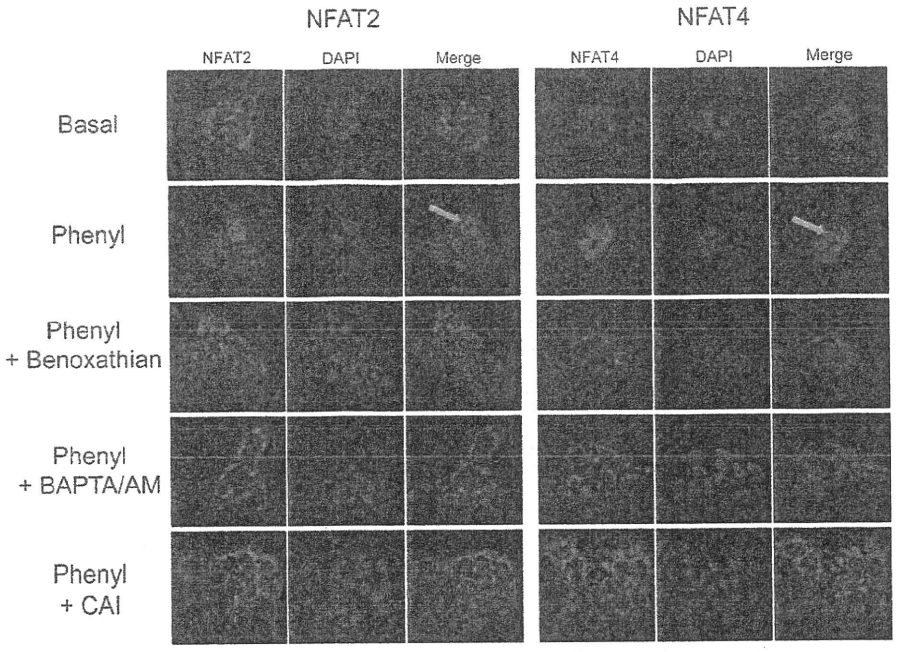

Fig. 5. Phenylephrine stimulates the nuclear translocation of NFAT2 and NFAT4. Immortalized small cholangiocytes were stimulated with phenylephrine in the presence/absence of benoxathian, BAPTA/AM, and CAI for 60 minutes. By immunofluorescence, phenylephrine stimulates the nuclear translocation of NFAT2 and NFAT4 (arrows), which was blocked by benoxathian, BAPTA/AM, and CAI. Original magnification, ×60.

there are no commercially available kits). Our results demonstrate that phenylephrine stimulates NFAT2 DNA-binding activity in small cholangiocytes, which was blocked by BAPTA/AM and CAI (Fig. 7A). We also found that phenylephrine stimulates the time-dependent increase in Sp1 DNA-binding activity in small cholangiocytes as determined by EMSA (Fig. 7B). The DNA-binding specificity of Sp1 when challenged during cold competition was determined and presented in Supporting Information Fig. 3. Because both Sp1 and Sp3 are known to interact with NFAT2 and NFAT4, we determined by DNA-binding activity ELISA which isoforms (i.e., Sp1 and Sp3) are activated by phenylephrine. In small immortalized cholangiocytes, phenylephrine stimulated Sp1 (but not Sp3), which was blocked by BAPTA/AM, CAI, and MiA (Fig. 7B,C).

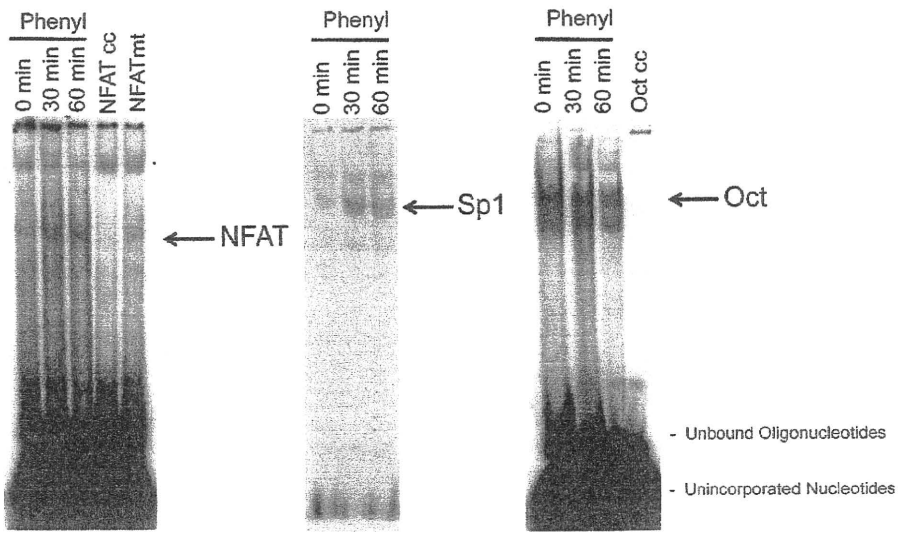

Fig. 6. Evaluation of phenylephrine-induced NFAT and Sp1 DNA-binding activity by EMSA. Immortalized small cholangiocytes were stimulated with phenylephrine for 0, 30, and 60 minutes at 37°C and DNA-binding activity was assessed by EMSA. Phenylephrine stimulated a time-dependent increase in DNA-binding for both NFAT (NFAT2 and 4 can both bind the consensus sequence) and Sp1. DNA-binding activity to the Oct consensus sequence was used as a loading control. Specificity of binding was demonstrated by adding 50-fold excess of either unlabeled NFAT consensus sequence, (NFAT cc), mutated NFAT consensus sequence (NFAT mt), or Oct sequence to the nuclear extract taken at time 0. NFAT = nuclear factor of activated T cells; NFAT cc = NFAT cold consensus sequence; NFAT mt = NFAT mutated competitor; Oct = octamer binding factor; and Oct cc = Oct cold consensus sequence.

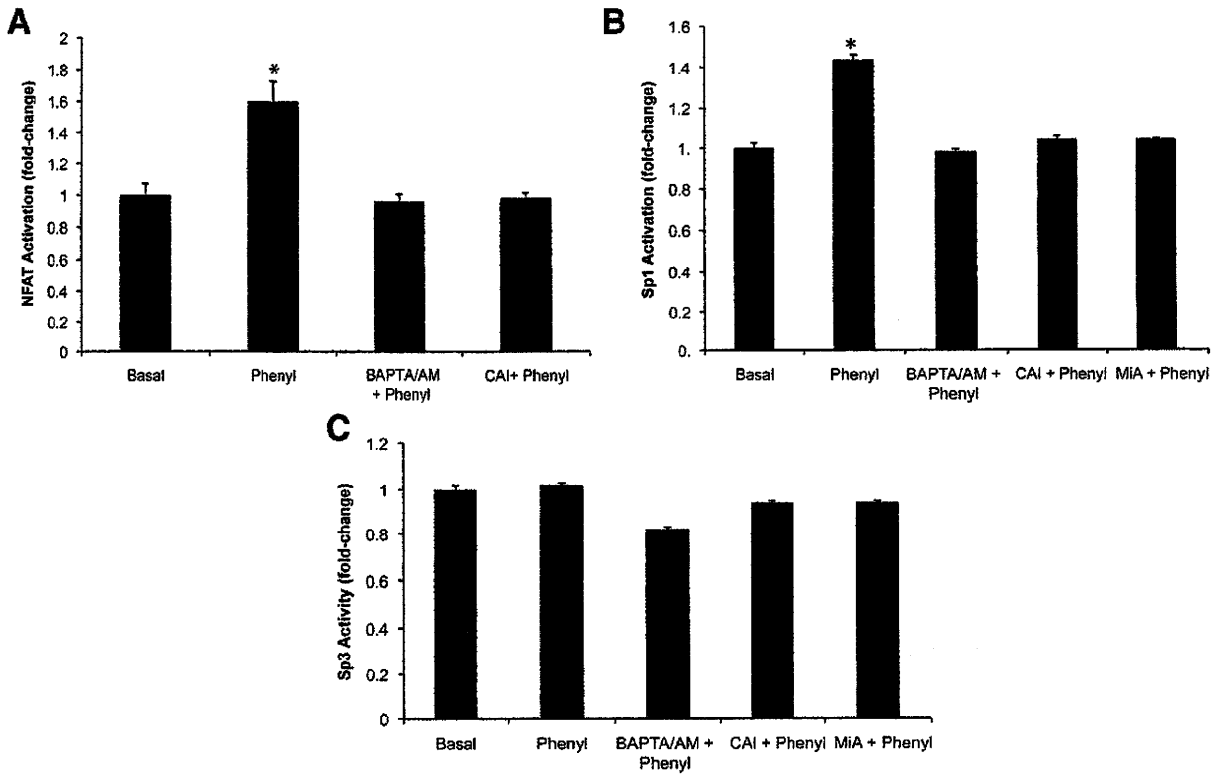

Fig. 7. Phenylephrine induces NFAT2 and Sp1 (but not Sp3) DNA-binding activity. (A) Immortalized small cholangiocytes were stimulated with phenylephrine in the presence/absence of BAPTA/AM and CAI for 60 minutes. NFAT2 DNA-binding activity was determined by ELISA. Phenylephrine stimulates the DNA-binding activity of NFAT2, which is blocked by BAPTA/AM and CAI. Asterisk (*) denotes significance ($P < 0.05$) when compared with the respective basal treatment using a t test ($n = 4$). (B,C) Small cholangiocytes were stimulated with phenylephrine in the presence/absence of BAPTA/AM, CAI and MiA for 60 minutes. Sp1 and Sp3 DNA-binding activity was determined by ELISA. Phenylephrine stimulates the DNA-binding activity of Sp1 (B), but not Sp3 (C), which is blocked by BAPTA/AM, CAI, and MiA. Asterisk (*) denotes significance ($P < 0.05$) when compared with the respective basal treatment using a t test ($n = 4$).

Knockdown of NFAT2 and Sp1 Expression in Immortalized Small Cholangiocytes Prevents Phenylephrine-Induced Proliferation. We established small cholangiocyte lines that have NFAT2, NFAT4, and Sp1 expression stably knockdown. Knockdown of NFAT2 expression prevented phenylephrine stimulated proliferation of small cholangiocytes (Fig. 8A). Knockdown of NFAT4 only slightly depressed phenylephrine-stimulated proliferation of small cholangiocytes (Fig. 8B). In NFAT4 knockdown cells, phenylephrine stimulated a significant increase in small cholangiocyte proliferation versus basal (Fig. 8B). Phenylephrine had no effect on small cholangiocyte proliferation in cells with knockdown of Sp1 expression (Fig. 8B).

Discussion

We demonstrated that: (1) small and large bile ducts and freshly isolated and immortalized cholangiocytes express all of the AR subtypes; (2) NFAT2 and NFAT4 are predominantly expressed by small bile ducts and immortalized small cholangiocytes; (3) phenylephrine stimulates both *in vivo* and *in vitro* the proliferation of small cholangiocytes via activation of Ca^{2+}-dependent signaling, which is blocked by *in vivo* and *in vitro* inhibition of NFAT and Sp1; (4) phenylephrine stimulates Ca^{2+}-dependent DNA-binding activities of NFAT2 and Sp1 (but not Sp3) and nuclear translocation of NFAT2 and NFAT4 in immortalized small cholangiocytes; and (5) knockdown of NFAT2 or Sp1 gene expression prevents phenylephrine-induced small cholangiocyte proliferation, whereas NFAT4 knockdown had a minimal effect on phenylephrine-induced proliferation of immortalized small cholangiocytes. The regulation of small cholangiocyte proliferation (via activation of α_{1A}, α_{1B}, α_{1D} AR by phenylephrine) is dependent on activation of Ca^{2+}/NFAT2/Sp1 signaling mechanisms.

The possible influence on the results by using small and large immortalized cholangiocytes are minimal, because these cells are derived from small and large

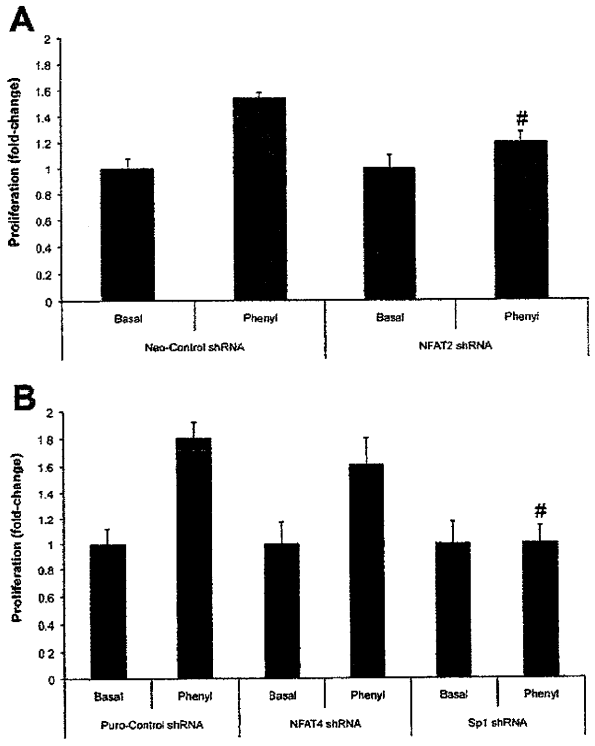

Fig. 8. Knockdown of NFAT2 and Sp1 expression prevents phenylephrine-induced proliferation of immortalized small cholangiocytes. The expression of NFAT2, NFAT4, or Sp1 was knockdown in small cholangiocytes by stable transfection of the respective shRNA. The knockdown of NFAT2 (A) and Sp1 (B) resulted in the prevention of phenylephrine-stimulated small cholangiocyte proliferation. (B) Knockdown of the expression NFAT4 did not significantly inhibit phenylephrine stimulation of small cholangiocyte proliferation. Data was expressed as fold-change relative to the respective basal values. Hash mark (£) denotes significance ($P < 0.05$) when compared with the respective phenyl-stimulated treatment group using a t test ($n = 7$).

bile ducts[5,6]; and have similar morphological, phenotypical and functional characteristics of freshly isolated small and large murine cholangiocytes.[5,6,35] These cell preparations express similar levels of the biliary markers, cytokeratin-7 and cytokeratin-19,[5,6] and display similar morphological differences in size.[5,6] At the functional level immortalized large (but not small) cholangiocytes express secretin receptor, CFTR and Cl^-/HCO_3-exchanger and selectively respond to secretin with changes in cAMP levels similar to that of freshly isolated cholangiocytes.[5,6] Immortalized small and large cholangiocytes display proliferative capacities similar to freshly isolated small and large mouse cholangiocytes because large cholangiocytes proliferate by a cAMP-dependent pathway, whereas IP_3/Ca^{2+}-dependent signalings regulate the growth of small cholangiocytes.[5,6,15] These findings support the validity of immortalized small and large cholangiocytes for evaluating functions of small and large bile ducts.

Small and large cholangiocytes express α_1-AR (α_{1A}, α_{1B}, α_{1D}). However, only immortalized small cholangiocytes respond *in vitro* to phenylephrine with increased proliferation that was blocked by all three α_1-AR antagonists (Fig. 4C). Although dobutamine induced *in vitro* a significant increase in the proliferation of immortalized small cholangiocytes, we did not address the mechanisms of such increase because dobutamine is a racemic mixture, in which one enantiomer is an agonist at β1 and β2 AR, and the other enantiomer is an agonist at α_1 AR.[36] Thus, dobutamine-induced increases in small cholangiocyte proliferation may be due to the activation of α_1 AR. A specific β1-AR agonist is not available. We have demonstrated that phenylephrine increases secretin-induced choleresis of large cholangiocytes when administered to bile duct–ligated rats.[10] In *in vitro* studies, phenylephrine did not alter basal but increased secretin-stimulated large bile duct secretory activity and cAMP levels, which were blocked by BAPTA/AM and Gö6976 (a PKC antagonist).[10] Phenylephrine increased IP_3 and Ca^{2+} levels and activated PKCα and PKCβ_{II}.[10] Because large cholangiocytes are normally hormonally responsive to secretin[16,37] and regulated by cAMP-dependent signaling,[3,16,23] we propose that this acute effect of phenylephrine on secretin-stimulated large bile duct secretion is likely mediated by activation of the Ca^{2+}-dependent adenylyl cyclase, AC8, which is key in the secretory activity of large cholangiocytes.[38] We postulated that phenylephrine has differential effects on small and large cholangiocytes. In immortalized small cholangiocytes, phenylephrine stimulated intracellular IP_3 levels and plays a role in stimulating proliferation. Activation of small cholangiocyte proliferation by endogenous catecholamines (such as, norepinephrine and epinephrine) and other Ca^{2+} agonists (including phenylephrine) may be key during pathological conditions when large cholangiocytes are damaged, and the *de novo* proliferation of small cholangiocytes is necessary for the replenishment of the biliary system and compensation for loss of hormonal responsiveness.[3,7] Other studies have shown that α_1-AR agonists like phenylephrine can induce proliferation in various cell types including hepatocytes.[39] We found a similar profile in small cholangiocytes, because phenylephrine-induced proliferation was blocked by inhibition of Ca^{2+}, calcineurin activity, and NFAT activity. In addition, phenylephrine-induced proliferation was blocked by MiA implicating the involvement of Sp1/3.

NFAT and Sp1/3 isoforms play a critical role in the regulation of cell proliferation. NFAT2 stimulates proliferation of several cell types including lymphocytes.[40] NFAT4 deficiency results in incomplete liver regeneration following partial hepatectomy.[41] NFAT2 and 4 have also been shown to crosstalk with Sp1/Sp3 to cooperatively regulate membrane type 1 matrix metalloproteinase gene transcription and cellular differentiation in keratinocytes.[42] Using several molecular approaches, we found that phenylephrine stimulates the Ca^{2+}-dependent DNA-binding activities of NFAT2/4, and Sp1 (but not Sp3) and the nuclear translocation of NFAT2 and NFAT4 suggesting the involvement of these transcription factors in phenylephrine-induced proliferation of small cholangiocytes. We confirmed their involvement using shRNA to knockdown the expression of these transcription factors.

In summary, we demonstrated that small cholangiocyte proliferation is regulated by the activation of α_1-ARs and occurs through Ca^{2+}/calcineurin-dependent activation of NFAT2 and Sp1. Modulation of the Ca^{2+}-dependent transcription factors, NFAT2 and SP1, may be an important therapeutic approach for inducing ductular proliferation for maintaining the homeostasis of the biliary during the damage of large cAMP-responsive bile ducts.[1,3,7]

Acknowledgment: We thank Anna Webb of the Texas A&M Health Science Center Microscopy Imaging Center for assistance with confocal microscopy and Bryan Moss (Medical Illustration, Scott & White) for the help on the preparation of the figures and Dr. Marco Marzioni (Università Politecnica delle Marche, Italy) for the comments related to the revision of the manuscript.

References

1. Alpini G, Prall RT, LaRusso NF. The pathobiology of biliary epithelia. In: Arias IM, Boyer JL, Chisari FV, Fausto N, Jakoby W, Schachter D, et al. eds. The Liver: Biology and Pathobiology, 4th ed. Philadelphia, PA: Lippincott Williams & Wilkins; 2001:421-435.
2. Alpini G, Glaser S, Ueno Y, Pham L, Podila PV, Caligiuri A, et al. Heterogeneity of the proliferative capacity of rat cholangiocytes after bile duct ligation. Am J Physiol Gastrointest Liver Physiol 1998;274: G767-G775.
3. LeSage G, Glaser S, Marucci L, Benedetti A, Phinizy JL, Rodgers R, et al. Acute carbon tetrachloride feeding induces damage of large but not small cholangiocytes from BDL rat liver. Am J Physiol Gastrointest Liver Physiol 1999;276:G1289-G1301.
4. Francis H, Glaser S, Ueno Y, LeSage G, Marucci L, Benedetti A, et al. cAMP stimulates the secretory and proliferative capacity of the rat intrahepatic biliary epithelium through changes in the PKA/Src/MEK/ERK1/2 pathway. J Hepatol 2004;41:528-537.
5. Ueno Y, Alpini G, Yahagi K, Kanno N, Moritoki Y, Fukushima K, et al. Evaluation of differential gene expression by microarray analysis in small and large cholangiocytes isolated from normal mice. Liver Int 2003;23:449-459.
6. Francis H, Glaser S, DeMorrow S, Gaudio E, Ueno Y, Venter J, et al. Small mouse cholangiocytes proliferate in response to H1 histamine receptor stimulation by activation of the IP3/CAMK I/CREB pathway. Am J Physiol Cell Physiol 2008;295:C499-C513.
7. Mancinelli R, Franchitto A, Gaudio E, Onori P, Glaser S, Francis H, et al. After damage of large bile ducts by gamma-aminobutyric acid, small ducts replenish the biliary tree by amplification of calcium-dependent signaling and de novo acquisition of large cholangiocyte phenotypes. Am J Pathol Gastrointest Liver Physiol 2010;176:1790-1800.
8. Francis H, LeSage G, DeMorrow S, Alvaro D, Ueno Y, Venter J, et al. The alpha2-adrenergic receptor agonist UK 14,304 inhibits secretin-stimulated ductal secretion by downregulation of the cAMP system in bile duct-ligated rats. Am J Physiol Cell Physiol 2007;293:C1252-C1262.
9. Glaser S, Alvaro D, Francis H, Ueno Y, Marucci L, Benedetti A, et al. Adrenergic receptor agonists prevent bile duct injury induced by adrenergic denervation by increased cAMP levels and activation of Akt. Am J Physiol Gastrointest Liver Physiol 2006;290:G813-G826.
10. LeSage G, Alvaro D, Glaser S, Francis H, Marucci L, Roskams T, et al. Alpha-1 adrenergic receptor agonists modulate ductal secretion of BDL rats via Ca(2+)- and PKC-dependent stimulation of cAMP. HEPATOLOGY 2004;40:1116-1127.
11. Hein P, Michel MC. Signal transduction and regulation: are all alpha1-adrenergic receptor subtypes created equal? Biochem Pharmacol 2007; 73:1097-1106.
12. Nguyen T, Di Giovanni S. NFAT signaling in neural development and axon growth. Int J Dev Neurosci 2008;26:141-145.
13. Lipskaia L, Lompre AM. Alteration in temporal kinetics of Ca2+ signaling and control of growth and proliferation. Biol Cell 2004;96: 55-68.
14. Ho SN. The role of NFAT5/TonEBP in establishing an optimal intracellular environment. Arch Biochem Biophys 2003;413:151-157.
15. Glaser S, Gaudio E, Rao A, Pierce LM, Onori P, Franchitto A, et al. Morphological and functional heterogeneity of the mouse intrahepatic biliary epithelium. Lab Invest 2009;89:456-469.
16. Alpini G, Roberts S, Kuntz SM, Ueno Y, Gubba S, Podila PV, et al. Morphological, molecular, and functional heterogeneity of cholangiocytes from normal rat liver. Gastroenterology 1996;110:1636-1643.
17. Alpini G, Ulrich C, Roberts S, Phillips JO, Ueno Y, Podila PV, et al. Molecular and functional heterogeneity of cholangiocytes from rat liver after bile duct ligation. Am J Physiol Gastrointest Liver Physiol 1997; 272:G289-G297.
18. Marinese D, Patel R, Walden PD. Mechanistic investigation of the adrenergic induction of ventral prostate hyperplasia in mice. Prostate 2003;54:230-237.
19. Noguchi H, Matsushita M, Okitsu T, Moriwaki A, Tomizawa K, Kang S, et al. A new cell-permeable peptide allows successful allogeneic islet transplantation in mice. Nat Med 2004;10:305-309.
20. Jia Z, Gao Y, Wang L, Li Q, Zhang J, Le X, et al. Combined treatment of pancreatic cancer with mithramycin A and tolfenamic acid promotes Sp1 degradation and synergistic antitumor activity. Cancer Res 2010;70:1111-1119.
21. LeSage G, Glaser S, Gubba S, Robertson WE, Phinizy JL, Lasater J, et al. Regrowth of the rat biliary tree after 70% partial hepatectomy is coupled to increased secretin-induced ductal secretion. Gastroenterology 1996;111:1633-1644.
22. Onori P, Wise C, Gaudio E, Franchitto A, Francis H, Carpino G, et al. Secretin inhibits cholangiocarcinoma growth via dysregulation of the cAMP-dependent signaling mechanisms of secretin receptor. Int J Cancer 2010;127:43-54.
23. Francis H, Franchitto A, Ueno Y, Glaser S, DeMorrow S, Venter J, et al. H3 histamine receptor agonist inhibits biliary growth of BDL rats by downregulation of the cAMP-dependent PKA/ERK1/2/ELK-1 pathway. Lab Invest 2007;87:473-487.
24. Oriowo MA, Chapman H, Kirkham DM, Sennitt MV, Ruffolo RR Jr, Cawthorne MA. The selectivity in vitro of the stereoisomers of the beta-3 adrenoceptor agonist BRL 37344. J Pharmacol Exp Ther 1996; 277:22-27.

25. Jia Z, Zhang J, Wei D, Wang L, Yuan P, Le X, et al. Molecular basis of the synergistic antiangiogenic activity of bevacizumab and mithramycin A. Cancer Res 2007;67:4878-4885.
26. Ford AP, Arredondo NF, Blue DR Jr, Bonhaus DW, Jasper J, Kava MS, et al. RS-17053 (N-[2-(2-cyclopropylmethoxyphenoxy)ethyl]-5-chloro-alpha, alpha-dimethyl-1H-indole-3-ethanamine hydrochloride), a selective alpha 1A-adrenoceptor antagonist, displays low affinity for functional alpha 1-adrenoceptors in human prostate: implications for adrenoceptor classification. Mol Pharmacol 1996;49:209-215.
27. Morton JS, Daly CJ, Jackson VM, McGrath JC. α1A-Adrenoceptors mediate contractions to phenylephrine in rabbit penile arteries. Br J Pharmacol 2007;150:112-120.
28. Goetz AS, King HK, Ward SD, True TA, Rimele TJ, Saussy DLJ. BMY is 7378 is a selective antagonist of the D subtype of alpha 1-adrenoceptors. Eur J Pharmacol 1995;272:R5-R6.
29. Ma P, Wang Z, Pflugfelder SC, Li DQ. Toll-like receptors mediate induction of peptidoglycan recognition proteins in human corneal epithelial cells. Exp Eye Res 2010;90:130-136.
30. Goodenough S, Davidson M, Chen W, Beckmann A, Pujic Z, Otsuki M, et al. Immediate early gene expression and delayed cell death in limbic areas of the rat brain after kainic acid treatment and recovery in the cold. Exp Neurol 1997;145:451-461.
31. Fuchs R, Stelzer I, Haas HS, Leitinger G, Schauenstein K, Sadjak A. The alpha1-adrenergic receptor antagonists, benoxathian and prazosin, induce apoptosis and a switch towards megakaryocytic differentiation in human erythroleukemia cells. Ann Hematol 2009;88:989-997.
32. Badran BM, Wolinsky SM, Burny A, Willard-Gallo KE. Identification of three NFAT binding motifs in the 5′-upstream region of the human CD3gamma gene that differentially bind NFATc1, NFATc2, and NF-kappa B p50. J Biol Chem 2002;277:47136-47148.
33. DeMorrow S, Francis H, Gaudio E, Ueno Y, Venter J, Onori P, et al. Anandamide inhibits cholangiocyte hyperplastic proliferation via activation of thioredoxin 1/redox factor 1 and AP-1 activation. Am J Physiol Gastrointest Liver Physiol 2008;294:G506-G519.
34. O-Uchi J, Komukai K, Kusakari Y, Obata T, Hongo K, Sasaki H, et al. alpha1-adrenoceptor stimulation potentiates L-type Ca2+ current through Ca2+/calmodulin-dependent PK II (CaMKII) activation in rat ventricular myocytes. Proc Natl Acad Sci U S A 2005;102:9400-9405.
35. Glaser S, Lam IP, Franchitto A, Gaudio E, Onori P, Chow BK, et al. Knockout of secretin receptor reduces large cholangiocyte hyperplasia in mice with extrahepatic cholestasis induced by bile duct ligation. HEPATOLOGY 2010;52:204-214.
36. Brunton L, Blumenthal D, Buxton I, Parker K. Goodman & Gilman's Manual of Pharmacology and Therapeutics. New York: McGraw-Hill Medical; 2008:159.
37. Alpini G, Glaser S, Robertson W, Rodgers RE, Phinizy JL, Lasater J, et al. Large but not small intrahepatic bile ducts are involved in secretin-regulated ductal bile secretion. Am J Physiol Gastrointest Liver Physiol 1997;272:G1064-G1074.
38. Strazzabosco M, Fiorotto R, Melero S, Glaser S, Francis H, Spirli C, et al. Differentially expressed adenylyl cyclase isoforms mediate secretory functions in cholangiocyte subpopulation. HEPATOLOGY 2009;50:244-252.
39. Han C, Bowen WC, Michalopoulos GK, Wu T. Alpha-1 adrenergic receptor transactivates signal transducer and activator of transcription-3 (Stat3) through activation of Src and epidermal growth factor receptor (EGFR) in hepatocytes. J Cell Physiol 2008;216:486-497.
40. Yoshida H, Nishina H, Takimoto H, Marengere LE, Wakeham AC, Bouchard D, et al. The transcription factor NF-ATc1 regulates lymphocyte proliferation and Th2 cytokine production. Immunity 1998;8:115-124.
41. Pierre KB, Jones CM, Pierce JM, Nicoud IB, Earl TM, Chari RS. NFAT4 deficiency results in incomplete liver regeneration following partial hepatectomy. J Surg Res 2009;154:226-233.
42. Santini MP, Talora C, Seki T, Bolgan L, Dotto GP. Cross talk among calcineurin, Sp1/Sp3, and NFAT in control of p21(WAF1/CIP1) expression in keratinocyte differentiation. Proc Natl Acad Sci U S A 2001;98:9575-9580.

Adenosine Triphosphate Release and Purinergic (P2) Receptor–Mediated Secretion in Small and Large Mouse Cholangiocytes

Kangmee Woo,[1] Meghana Sathe,[1] Charles Kresge,[1] Victoria Esser,[2] Yoshiyuki Ueno,[5] Julie Venter,[3] Shannon S. Glaser,[3] Gianfranco Alpini,[3,4] and Andrew P. Feranchak[1]

Adenosine triphosphate (ATP) is released from cholangiocytes into bile and is a potent secretogogue by increasing intracellular Ca^{2+} and stimulating fluid and electrolyte secretion via binding purinergic (P2) receptors on the apical membrane. Although morphological differences exist between small and large cholangiocytes (lining small and large bile ducts, respectively), the role of P2 signaling has not been previously evaluated along the intrahepatic biliary epithelium. The aim of these studies therefore was to characterize ATP release and P2-signaling pathways in small (MSC) and large (MLC) mouse cholangiocytes. The findings reveal that both MSCs and MLCs express P2 receptors, including P2X4 and P2Y2. Exposure to extracellular nucleotides (ATP, uridine triphosphate, or 2′,3′-O-[4-benzoyl-benzoyl]-ATP) caused a rapid increase in intracellular Ca^{2+} concentration and in transepithelial secretion (I_{sc}) in both cell types, which was inhibited by the Cl^- channel blockers 5-nitro-2-(-3-phenylpropylamino)-benzoic acid (NPPB) or niflumic acid. In response to mechanical stimulation (flow/shear or cell swelling secondary to hypotonic exposure), both MSCs and MLCs exhibited a significant increase in the rate of exocytosis, which was paralleled by an increase in ATP release. Mechanosensitive ATP release was two-fold greater in MSCs compared to MLCs. ATP release was significantly inhibited by disruption of vesicular trafficking by monensin in both cell types. *Conclusion:* These findings suggest the existence of a P2 signaling axis along intrahepatic biliary ducts with the "upstream" MSCs releasing ATP, which can serve as a paracrine signaling molecule to "downstream" MLCs stimulating Ca^{2+}-dependent secretion. Additionally, in MSCs, which do not express the cystic fibrosis transmembrane conductance regulator, Ca^{2+}-activated Cl^- efflux in response to extracellular nucleotides represents the first secretory pathway clearly identified in these cholangiocytes derived from the small intrahepatic ducts. (HEPATOLOGY 2010;52:1819-1828)

Cholangiocytes, the epithelial cells that form the intrahepatic bile ducts, represent an important component of the bile secretory unit. Although bile formation is initiated at the hepatocyte canalicular membrane, cholangiocytes subsequently modify the composition of bile through regulated ion secretion throughout the network of bile ducts.[1] Interestingly, secretory mechanisms along the intrahepatic bile ducts are not uniform. In all biliary models studied, including human, rat, and mouse bile ducts, cholangiocytes are known to be morphologically and functionally heterogeneous. Large cholangiocytes, from large ducts, express secretin receptors on the basolateral membrane and express cystic fibrosis transmembrane

Abbreviations: AE2, anion exchanger 2; ATP, adenosine triphosphate; Bz-ATP, 2′,3′-O-(4-benzoyl-benzoyl)-ATP; cAMP, cyclic adenosine monophosphate; CFTR, cystic fibrosis transmembrane conductance regulator; fura-2-AM, fura-2-acetoxymethyl ester; IP3, inositol 1,4,5-triphosphate; Isc, transepithelial short-circuit current response; MLC, mouse large cholangiocyte; MSC, mouse small cholangiocyte; NPPB, 5-nitro-2-(-3-phenylpropylamino)-benzoic acid; RT-PCR, reverse transcription polymerase chain reaction; UTP, uridine triphosphate.

From the [1]Department of Pediatrics, and [2]Internal Medicine, University of Texas Southwestern Medical Center, Dallas, TX; [3]Research, Central Texas Veterans Health Care System, Scott & White Digestive Disease Research Center, Scott & White Healthcare, Temple, TX; [4]Department of Medicine, Division Gastroenterology, Texas A&M Health Science Center College of Medicine, Temple, TX; and [5]Tohoku University, School of Medicine, Sendai, Japan.

Received September 21, 2009; accepted July 22, 2010.

This study was supported by the Cystic Fibrosis Foundation (FERANC08G0), the Children's Medical Center Foundation, and the National Institute of Diabetes, Digestive and Kidney Diseases (NIDDK) of the National Institutes of Health, grants DK078587 (to A.P.F.) and DK054811 (to G.A.), and a VA Merit Award (to G.A.).

conductance regulator (CFTR) and the HCO_3^-/Cl^- anion exchanger 2 (AE2) on the apical membrane,[2-4] and hence respond to secretin with an increase in [cAMP] (intracellular cyclic adenosine monophosphate concentration), and subsequent Cl^- and HCO_3^- efflux into the lumen. Conversely, small cholangiocytes, from small ducts, do not express secretin receptors, CFTR, or HCO_3^-/Cl^- exchanger and do not exhibit a secretory response to secretin.[3] In human liver, parallel to the findings observed in the rat and mouse, secretin-stimulated duct secretory activity is heterogeneous, because only medium and large interlobular bile ducts express the Cl^-/HCO_3^- exchanger AE2.[5]

Recently, secretion mediated by extracellular nucleotides (e.g., adenosine triphosphate [ATP]) acting on purinergic (P2) receptors on the luminal membrane of biliary epithelial cells has emerged as functionally important. ATP is present in bile,[6] and binding of ATP to P2 receptors increases K^+,[7,8] and Cl^- efflux from isolated cholangiocytes[9,10] and dramatically increases transepithelial secretion in biliary epithelial monolayers.[10,11] Indeed, the magnitude of the secretory response to ATP is two-fold to three-fold greater than that to cAMP.[10] Interestingly, recent evidence suggests that even cAMP-stimulated bile flow is mediated by ATP release into the duct lumen and stimulation of apical P2 receptors.[12] Together, these studies challenge and extend the conventional model that centers on the concept that cAMP-dependent opening of CFTR-related Cl^- channels is the driving force for cholangiocyte secretion. Rather, the operative regulatory pathways appear to take place within the lumen of intrahepatic ducts, where release of ATP into bile is a final common pathway controlling ductular bile formation. In light of recent studies demonstrating that the mechanical effects of fluid-flow or shear stress at the apical membrane of biliary epithelial cells is a robust stimulus for ATP release,[13] a model emerges in which mechanosensitive ATP release and Cl^- secretion is a dominant pathway regulating biliary secretion.

Although cholangiocytes express a repertoire of both P2X and P2Y receptors,[11,14,15] it is unknown if expression differs between small and large cholangiocytes and/or if functional differences exist in ATP release and signaling along the bile duct. The aim of the current studies therefore was to determine if a potential P2 signaling axis may exist along the bile duct by evaluating mechanosensitive ATP release and exocytosis, P2 receptor expression and function, and secretion mediated by extracellular nucleotides in both small (MSC) and large (MLC) mouse cholangiocytes.

Materials and Methods

Cell Models. Studies were performed in mouse cholangiocytes isolated from normal mice (BALB/c) and immortalized by transfection with the simian virus 40 large-T antigen gene.[4] These cells demonstrate identical properties to freshly isolated small and large mouse cholangiocytes.[3] Cells were maintained in culture as described.[3,4] Additional studies of P2 receptor expression were performed in primary cholangiocytes isolated from C57BL/6 mice (Charles River, Wilmington, MA) as previously described.[16,17] All animal experiments were performed in accordance with a protocol approved by the Scott & White Institutional Animal Care and Use Committee and in accordance with the Guide for the Care and Use of Laboratory Animals published by the U.S. National Institutes of Health (NIH Publication No. 85-23, revised 1996).

Total RNA Isolation and RT-PCR Analysis. Total RNA was extracted using TRIZOL Reagent (Invitrogen, Carlsbad, CA) and 1 μg RNA was reverse transcribed in the presence of 100 pmol oligo-deoxythymidine primer. For reverse transcription polymerase chain reaction (RT-PCR), aliquots of 5% of the total complementary DNA were amplified with TaqDNA polymerase in a reaction mixture containing 20 pmol of 5′ and 3′ primers specifically designed for various P2X and P2Y receptors (Supporting Information Methods and Supporting Information Table 1).

Measurement of Intracellular Ca^{2+} Concentration. MLCs and MSCs were grown to confluence on coverglass (Fig. 2), loaded with 2.5 μg/mL of fura-2-acetoxymethyl ester (fura-2-AM; TEF Laboratories, Austin, TX), placed in a perfusion chamber (RC-25F/PHA; Warner Instruments) on the stage of an inverted fluorescence microscope (Nikon TE2000), and the inflow and outflow ports were connected to a syringe pump. Changes of $[Ca^{2+}]_i$ (the intracellular calcium

Address reprint requests to: Andrew P. Feranchak, M.D., UT Southwestern Medical Center, 5323 Harry Hines Boulevard, Dallas, TX 75390-9063. E-mail: drew.feranchak@UTSouthwestern.edu; fax: 214-648-2673.

View this article online at wileyonlinelibrary.com.
DOI 10.1002/hep.23883
Potential conflict of interest: Nothing to report.
Additional Supporting Information may be found in the online version of this article.

concentration) were measured at excitation wavelength of 340 nm (calcium-bound fura-2-AM) and 380 nm (calcium-free fura-2-AM), and emission wavelength of 510 nm and $[Ca^{2+}]_i$ was calculated.

Immunostaining. Confluent MSCs and MLCs were incubated with acetylated α-tubulin antibody (Sigma), as a marker for the primary cilium, and rhodamine phalloidin (Invitrogen) to label actin. Imaging was performed using a PerkinElmer UltraVIEW ERS spinning disk confocal microscope (PerkinElmer, Boston, MA). Imaris 5.0 (Bitplane, Inc., Saint Paul, MN) was used for three-dimensional volume rendering of z-stacks.

Measurement of Exocytosis. Exocytosis was assessed by real time imaging using the fluorescent dye FM1-43 (Molecular Probes, Inc., Eugene, OR) as previously described.[18] FM1-43 is weakly fluorescent in aqueous solution, but its fluorescence increases >300-fold when it binds plasma membrane and, therefore, it is a useful dye for the measurement of increased plasma membrane due to fusion of vesicle membrane with the plasma membrane during exocytosis.

Measurement of ATP Release. Bulk ATP release was studied from confluent cells using the luciferin-luciferase (L-L) assay as previously described.[13,19,20] Cell swelling was induced by adding water to dilute media 33% and defined shear stress was applied to confluent cells in a parallel plate chamber. All luminescence values are reported as relative change from basal luminescence per total protein level in the sample (measured in micrograms per milliliter) to control for any potential differences in luciferase activity or confluency between samples, respectively. Detailed protocols for measurements of ATP release, ATP degradation, protein levels, and lactate dehydrogenase are described in Supporting Information Methods.

Transepithelial Cl− Secretion. MLCs and MSCs were grown on collagen-coated polycarbonate filters with a pore size of 0.4 μm (Costar, Cambridge, MA) and the transmembrane resistance was measured daily (Evohm voltmeter; World Precision Instruments, Sarasota, FL).[21] Filters were mounted in an Ussing chamber, filled with standard buffer solution, and transepithelial short-circuit current response (I_{sc}) was measured under 0 mV voltage-clamp conditions through agar bridges connected to Ag-AgCl electrodes using an epithelial voltage clamp amplifier (model EC-825; Warner Instruments, MRA International, Naples, FL). The I_{sc} represents the net sum of the transepithelial fluxes of anion and cation and the level of ion secretion.[11] Studies included paired, same-day monolayers to minimize any potential effects of day-to-day variability.

Reagents and Statistics. Detailed descriptions of the reagents, buffer solutions, experimental protocols, and statistical analysis are provided in Supporting Information Materials.

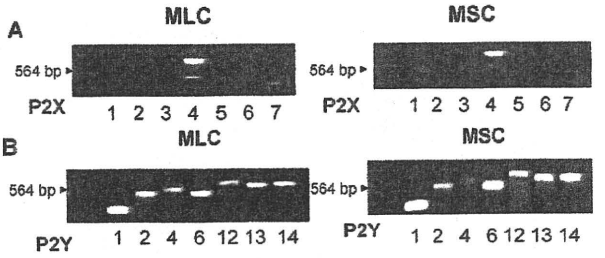

Fig. 1. Mouse cholangiocytes express P2 receptors. Molecular expression of P2X and P2Y receptor subtypes was evaluated by RT-PCR with specific oligonucleotides. (A) P2X receptor expression. P2X4 is the predominant P2X receptor in both mouse large (MLC), left panel, and mouse small (MSC), right panel, cholangiocytes. (B) P2Y receptor expression. Both MLCs and MSCs express multiple P2Y receptor subtypes, including P2Y1, P2Y2, P2Y4, P2Y6, P2Y12, P2Y13, and P2Y14. The arrowhead indicates a 564-base pair (bp) λDNA-Hind III fragment.

Results

Large and Small Cholangiocytes Express a Repertoire of P2X and P2Y Receptors. In both MLCs and MSCs, complementary DNAs were probed with oligonucleotide primers specific to the seven P2X subtypes and seven P2Y subtypes in mouse (shown in Supporting Information Table 1) and amplified using RT-PCR. Representative studies are shown in MLCs and MSCs (Fig. 1), and in primary isolated cholangiocytes (Supporting Information Fig. 1). In both MLCs and MSCs, clear bands corresponding to P2X4 and all seven P2Y receptors (P2Y1, P2Y2, P2Y4, P2Y6, P2Y11, P2Y12, and P2Y13) are present. These results are consistent with previous studies of human and rat biliary cells where a predominance of P2X4 and multiple P2Y receptors were observed.[11,14,15]

Agonist Profile of Nucleotide-Stimulated Ca^{2+} Fluorescence. To establish the functional significance of mouse cholangiocyte P2 receptor expression, MSCs and MLCs were grown to confluence (Fig. 2) and changes in Ca^{2+} fluorescence measured in response to P2Y and P2X agonists. Exposure to ATP, UTP, a P2Y-preferring agonist, or Bz-ATP, a P2X-preferring agonist, all resulted in significant increases in $[Ca^{2+}]_i$ in both MLCs and MSCs (Fig. 3). The ATP-stimulated increase in $[Ca^{2+}]_i$ was abolished by the P2Y receptor blocker, suramin (Fig. 3D). Together, these results demonstrate that P2X4 and P2Y receptors expressed by both MLCs and MSCs are functionally active. No differences were observed between MLCs and MSCs in either the magnitude or kinetics of the Ca^{2+} response to any of the nucleotides.

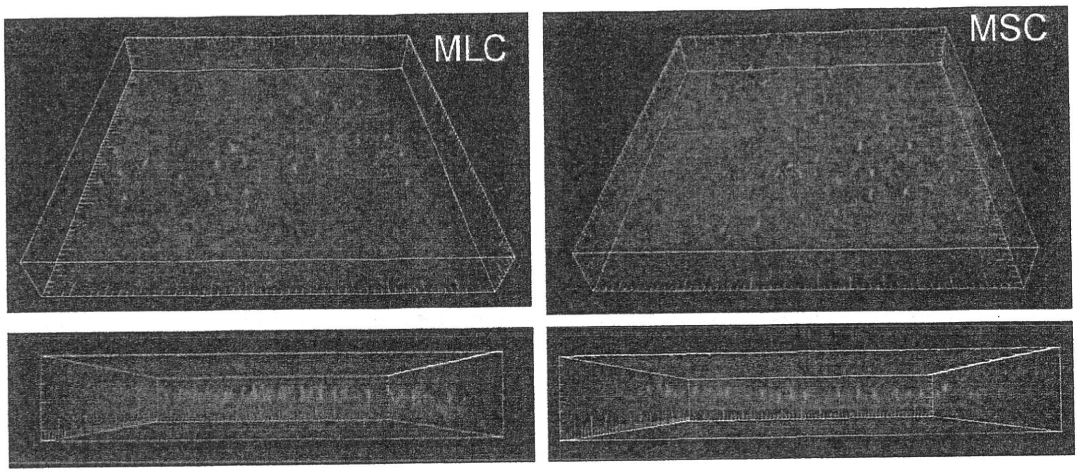

Fig. 2. MLCs and MSCs form polarized monolayers. MLCs (left) and MSCs (right) were cultured on coverglass for 5 days and stained for acetylated α-tubulin, as a cilia marker protein (green), and phalloidin, for actin localization (red). Bottom panels represent z axis to highlight cilia. Scale, small hatch marks = 5 μm.

Functional Role for P2 Receptors in Transepithelial Secretion. When cultured as described, both MSCs and MLCs developed an increase in transmembrane resistance by day 3 signifying the development of confluent monolayers with tight junctions (Fig. 4A). When mounted in an Ussing chamber, confluent MLCs and MSCs monolayers exhibited a basal I_{sc}, reflecting transepithelial secretion, which increased dramatically in response to the addition of ATP (100 μM) to the apical chamber (Fig. 4B,C). The nucleotide-stimulated I_{sc} was significantly inhibited by the nonspecific Cl^- channel blocker, 5-nitro-2-(-3-phenylpropylamino)-benzoic acid (NPPB), or by the Ca^{2+}-activated Cl^- channel blocker niflumic acid (Fig. 4C,F). Additionally, preincubation with the IP3 receptor blocker, 2-APB, significantly inhibited the ATP-stimulated increase in I_{sc} in both MLC and MSC (Fig. 4C). In separate experiments, the effect of apical versus basolateral P2 receptor stimulation on the I_{sc} was determined. For both MSCs and MLCs, an increase in the I_{sc} was observed when nucleotides were added to either chamber, consistent with functional expression of P2 receptors on both apical and basolateral membranes. The magnitude of the change in I_{sc} was similar

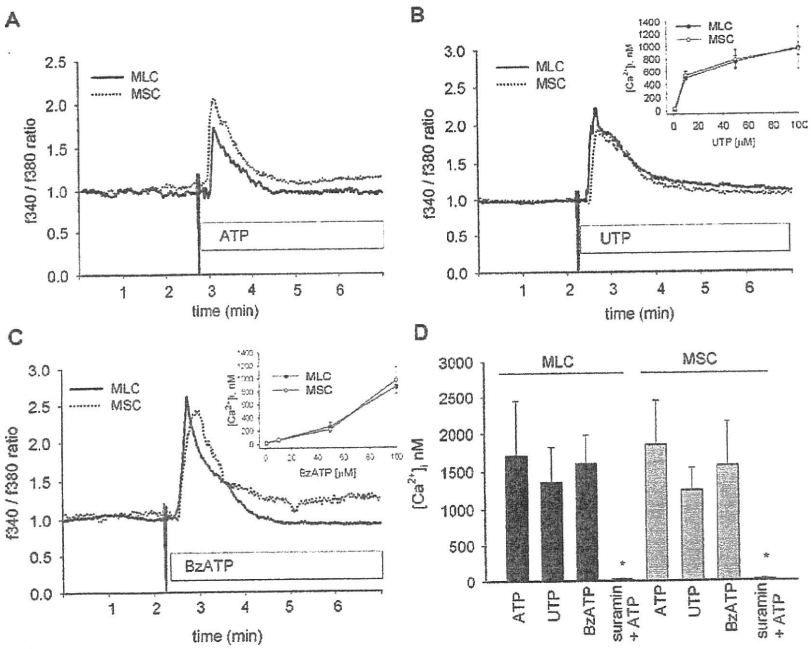

Fig. 3. P2 receptor agonists increase intracellular Ca^{2+} in mouse cholangiocytes. MLCs and MSCs were loaded with fura-2-AM and exposed to extracellular nucleotides, ATP (100 μM), UTP (100 μM), or Bz-ATP (100 μM) as indicated. The y axis values represent the ratio of fluorescence at 340 (f340) and at 380 nm (f380). (A-C) Representative studies. The Ca^{2+} fluorescence increased rapidly in both MLCs (solid line) and MSCs (dotted line) upon exposure to nucleotides. Insets in (B) and (C) demonstrate dose-response for respective agonist. (D) Cumulative data. Values represent the maximal $[Ca^{2+}]_i$ in nM. $[Ca^{2+}]_i$ was calculated based on maximal and minimal Ca^{2+} fluorescence obtained by exposure to ionomycin (5 μM) and EGTA (10 mM), respectively (N = 3-6 each). *Suramin significantly inhibits ATP-stimulated [Ca2+]i, $P < 0.05$.

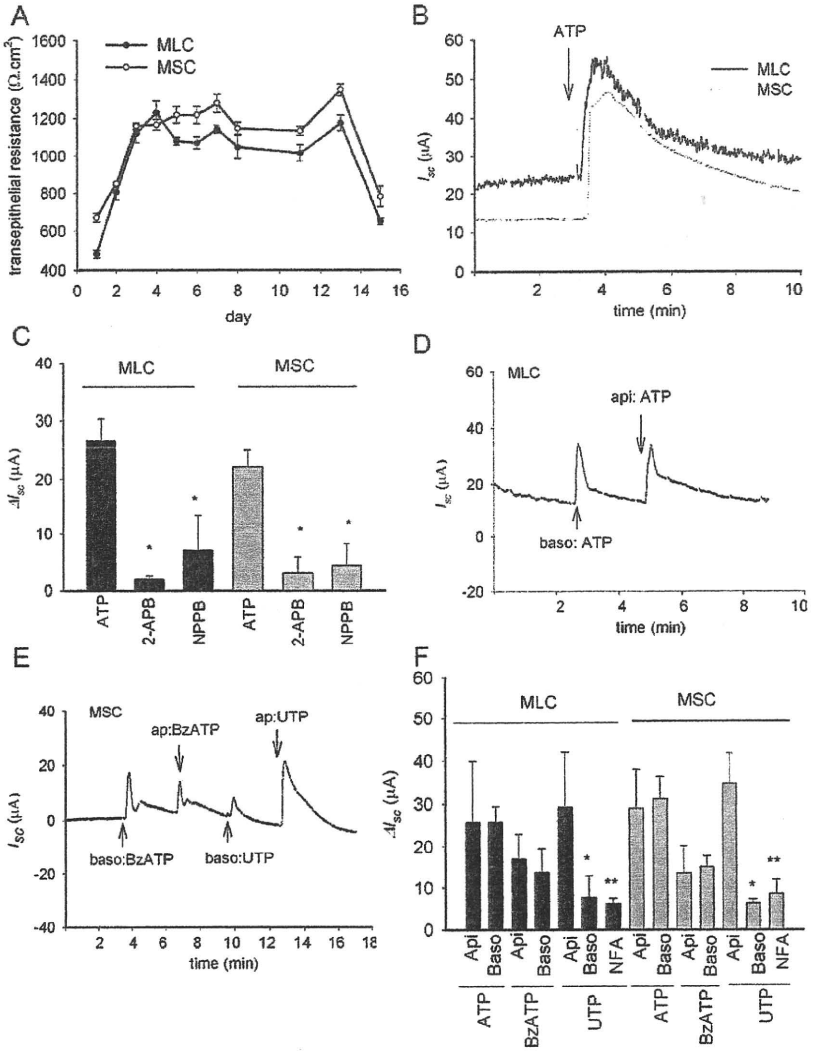

Fig. 4. Mouse cholangiocytes form polarized monolayers and exhibit increases in transepithelial Cl^- secretion in response to extracellular nucleotides. (A) Transmembrane resistance ($\Omega.cm^2$) was measured at the time points indicated in MLCs and MSCs grown on semipermeable filters. (B) Representative tracings of MLCs or MSCs mounted in an Ussing chamber. The *y* axis represents short-circuit current (I_{sc}) across monolayers measured under voltage-clamp conditions (μA). ATP (100 μM), added to the apical chamber, significantly increased I_{sc}. (C) Cumulative data demonstrating effect of 2-APB or NPPB on ATP-stimulated I_{sc}. The *y* axis values are reported as ΔI_{sc} (maximum I_{sc} − basal I_{sc}). *The 2-APB or NPPB significantly inhibit ATP-stimulated ΔI_{sc} ($P < 0.05$, n= 3-9 each). (D) Representative recording of apical or basolateral additions of ATP (100 μM)-stimulated I_{sc} in MLCs. (E) Representative recording of apical or basolateral additions of BzATP (100 μM) and UTP (100 μM) in MSCs. (F) Cumulative data. Values (mean ± standard error of the mean [SEM]) represent ΔI_{sc}. Apical addition (Api) and basolateral addition (Baso), of respective reagent (n = 4-12 each). *Apical addition of UTP increases I_{sc} > than basolateral addition ($P < 0.05$). **Niflumic acid (NFA, 250 μM) inhibits UTP-stimulated I_{sc} ($P < 0.05$).

when nucleotides were added to either apical or basolateral compartments for all nucleotides tested except for UTP which caused a significantly greater increase in I_{sc} when added apically versus basolateral addition. Thus, both MSCs and MLCs express functional P2 receptors on both apical and basolateral membranes. Nucleotide binding to P2 receptors causes an increase in $[Ca^{2+}]_i$, predominantly through an IP3 receptor-dependent mechanism, which stimulates Ca^{2+}-activated Cl^- channels, and results in transepithelial secretion. To our knowledge, these represent the first integrated I_{sc} measurements of transepithelial secretion in mouse cholangiocytes. Furthermore, in MSC, which do not express CFTR, Ca^{2+}-activated Cl^- efflux in response to extracellular nucleotides represents the first secretory pathway clearly identified in these cells derived from the small intrahepatic ducts.

Mechanosensitive ATP Release. In human biliary cells and normal rat cholangiocyte monolayers, mechanical stimulation,[22] shear stress,[13] and cell swelling secondary to hypotonic exposure,[22] have all been identified as significant stimuli for ATP release. Studies were performed to determine if these mechanical stimuli result in a similar increase in the magnitude of ATP release in mouse cholangiocytes. First, in response to hypotonic exposure (33% dilution) to stimulate cell swelling, a rapid and large increase in ATP release was observed in both MLCs and MSCs (Fig. 5A). The magnitude of the response, which peaked within 30 seconds, was significantly greater in MSCs versus MLCs (Fig. 5A,C). Separate studies were performed to assess the effects of shear on ATP release. Under low shear conditions (shear 0.08 dyne/cm^2) no increase in ATP release was observed; however, increasing shear to

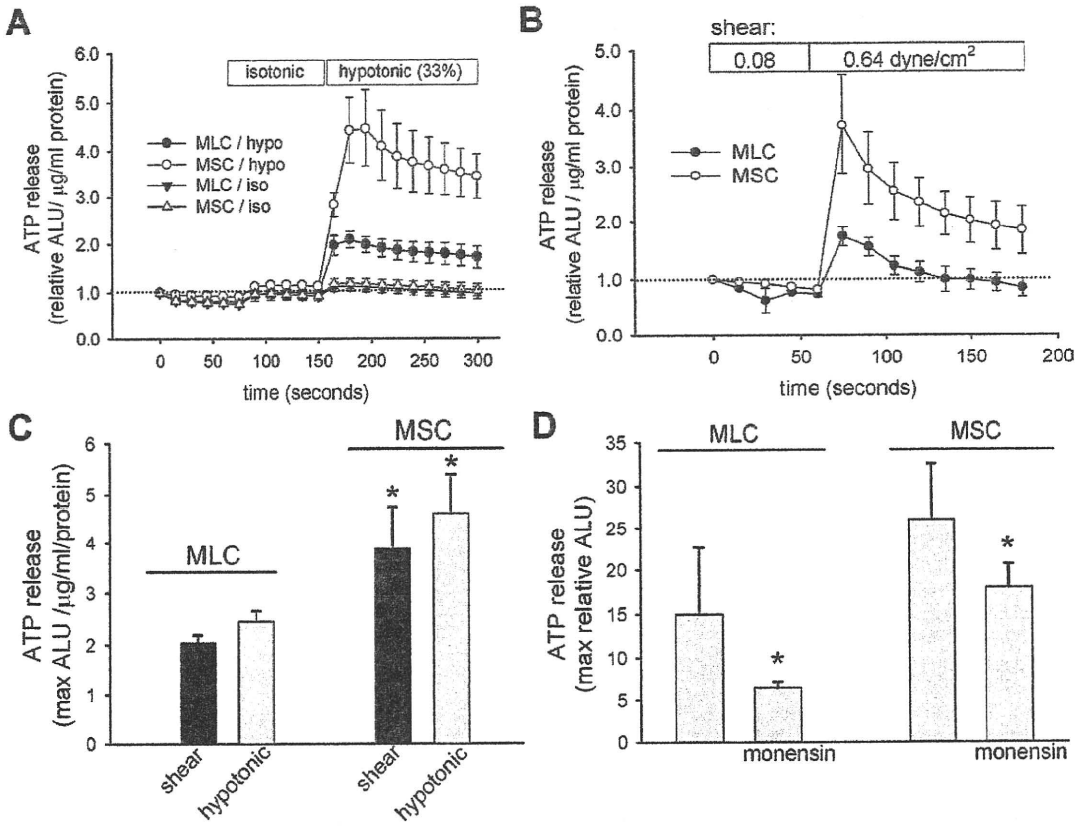

Fig. 5. Mechanosensitive ATP release from mouse cholangiocytes. ATP in the extracellular media was detected using the luciferin-luciferase assay and quantified as arbitrary light units (ALU). The *y* axis represents relative increase from basal luminescence (expressed as relative ALU/ μg/mL protein). (A) Cell swelling-induced ATP release from confluent MLCs and MSCs. Addition of isotonic media to cells led to a small increase in luminescence. Dilution of media 33% by the addition of water (indicated by bar) led to an increase in ATP release in both MSCs (open circles) and MLCs (closed circles) much greater than control cells exposed to only a second isotonic exposure. (B) Shear-stimulated ATP release from confluent MLCs (closed circles) and MSCs (open circles) cells. Cells were perfused with Optimem and 60 μL aliquots were taken from the efflux every 30 seconds, added to standard L-L reagent, and immediately placed in the Luminometer for luminescence measurement. Bars along top indicate length of low flow (shear 0.08 dyne/cm^2) and high flow (shear 0.64 dyne/cm^2) exposure. (C) Cumulative data demonstrating relative ATP release from both MLCs and MSCs in response to shear (0.64 dyne/cm^2, black bar) and hypotonic exposure (33% dilution, gray bar). Values represent maximum ATP concentration within 30 seconds of shear or hypotonic exposure, mean ± SEM. *ATP release is significantly greater in MSCs versus MLCs, $P < 0.05$. (D) Inhibition of vesicular trafficking inhibits swelling-induced ATP release in MLCs and MSCs. *Monensin (100 μM × 30 minutes) significantly inhibits ATP release in response to hypotonic exposure (33% dilution); $P < 0.05$, n = 4-6 each.

0.64 dyne/cm^2 caused a rapid relative increase in ATP release in both MLCs and MSCs, and again the magnitude of the peak response was significantly greater in MSCs versus MLCs ($P < 0.05$, Fig. 5B,C). No difference was noted in lactate dehydrogenase measurements before or after stimulus, for either hypotonic or shear exposure, excluding cell lysis as contributing to measured ATP (data not shown). In other biliary models, ATP release has been linked to exocytosis.[18] To determine if exocytosis contributes to ATP release in MLCs and MSCs, studies were performed in the presence or absence of monensin, a carboxylic ionophore known to dissipate the transmembrane pH gradients in Golgi and lysosomal compartments and disrupt vesicular trafficking. In both MLCs and MSCs, monensin significantly inhibited swelling-induced (33% hypotonic exposure) ATP release (Fig. 5D). Thus, both MSCs and MLCs exhibit mechanosensitive ATP release which is dependent on intact vesicular trafficking pathways. Additionally, the magnitude of mechanosensitive ATP release is significantly greater (~two-fold) in MSCs compared to MLCs.

Mechanosensitive Exocytosis. To determine if the difference in ATP release observed between MSCs and MLCs are the result of generalized differences in total cellular exocytosis, rates of exocytosis were measured in response to mechanical stimuli in both cell types. After equilibration with FM1-43, cells were exposed to hypotonic buffer (33%) which was associated with a rapid increase in fluorescence, reflecting an increase in

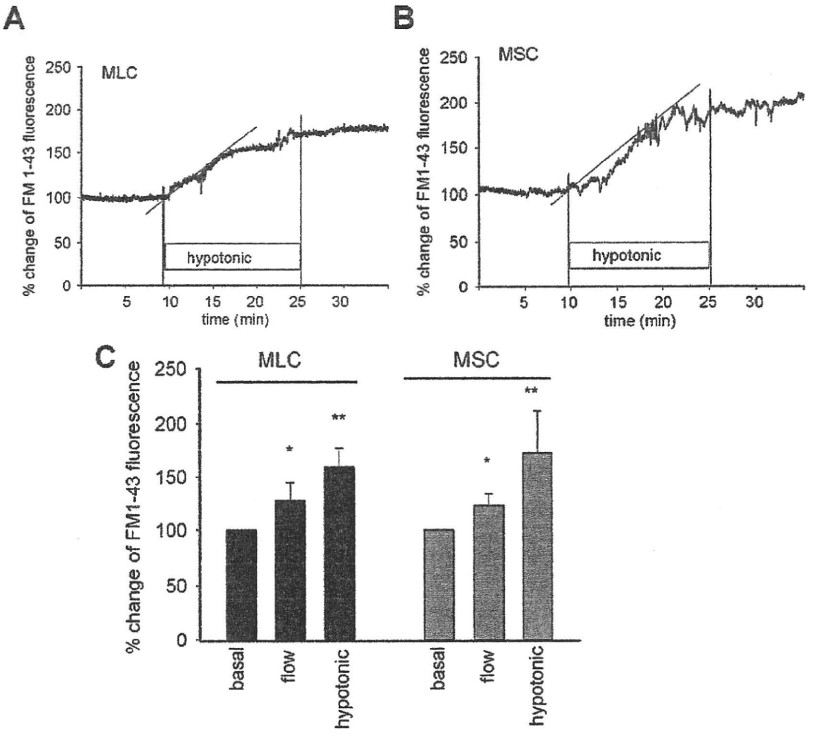

Fig. 6. Mechanosensitive exocytosis. MLCs and MSCs on coverglass were loaded with FM1-43 and exposed to shear or hypotonicity as indicated. The values of the *y* axis represent percent increase in membrane fluorescence. (A,B) Representative figures of swelling-induced exocytosis. FM1-43 fluorescence was stabilized in isotonic buffer before the cells were exposed to hypotonic buffer (33%). Hypotonic exposure rapidly increased plasma membrane fluorescence as a result of vesicular exocytosis in both (A) MLCs and (B) MSCs. Dotted line represents best-fit regression analysis. (E) Cumulative data demonstrating maximum magnitude of exocytosis in both MLCs and MSCs in response to shear (0.64 dyne/cm^2) or hypotonic (33%) exposure. Values represent maximum percent change in FM1-43 fluorescence (n = 5-6 each). *$P < 0.05$ shear versus basal; **$P < 0.05$ hypotonic exposure versus isotonic.

exocytosis (Fig. 6). In separate studies, exposure to shear (0.64 dyne/cm^2) also resulted in an increase in exocytosis (Fig. 6). These findings suggest a functional link between exocytosis and ATP release in both MLCs and MSCs. There was no significant difference noted in the rate or magnitude of exocytosis between MLCs and MSCs in response to either of these mechanical stimuli.

ATP Degradation. The concentration of extracellular ATP in bile is regulated not only through the rate of ATP release, but also through degradation pathways.[23] To determine if differences exist in the kinetics of ATP degradation between MSCs and MLCs, the media bathing confluent cells was loaded with exogenous ATP (10 nM). Changes in bioluminescence were monitored continuously until relative ALU returned to basal levels. As shown in Fig. 7, addition of ATP (10 nM) to MLCs increased relative bioluminescence 2.7-fold. The time course of degradation was described by a single exponential ($y = ae^{-0.038\ min}$, r = 0.99). By comparison, addition of ATP to MSCs increased bioluminescence 2.5-fold with a similar rate of degradation

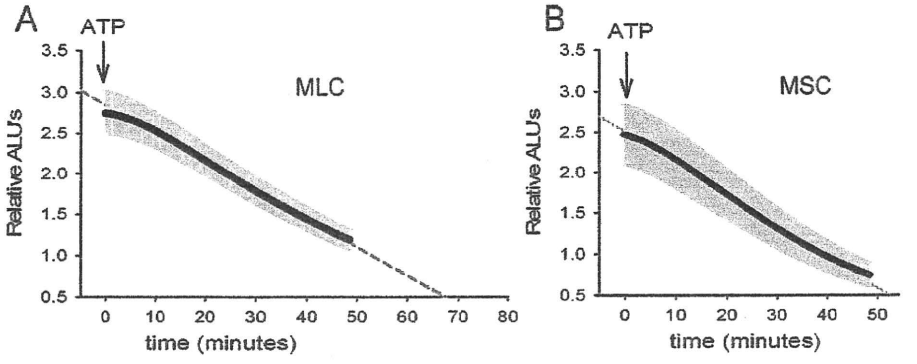

Fig. 7. Kinetics of ATP degradation in mouse cholangiocytes. ATP degradation was assessed after addition of ATP (10 nM, at arrow) to apical membrane of confluent (A) MLCs and (B) MSCs. The *y* axis represents relative arbitrary light units (ALU). Values represent means (black points) ± SEM (gray bars); n = 4 monolayers/time point. Dashed line represents best-fit regression.